

# Ediacaran obduction of a fore-arc ophiolite in SW Iberia: a turning point in the evolving geodynamic setting of peri-Gondwana

**Rubén Díez Fernández<sup>1</sup>, Alberto Jiménez-Díaz<sup>1,2</sup>, Ricardo Arenas<sup>3</sup>, M. Francisco Pereira<sup>4</sup>, Javier Fernández-Suárez<sup>3</sup>**

<sup>1</sup>*Departamento de Geodinámica, Estratigrafía y Paleontología (UCM), Universidad Complutense de Madrid. 28040 Madrid, Spain*

<sup>2</sup>*Instituto de Ciencias de la Tierra Jaume Almera, ICTJA, CSIC, 08028 Barcelona, Spain*

<sup>3</sup>*Departamento de Mineralogía y Petrología (UCM), Universidad Complutense de Madrid. 28040 Madrid, Spain*

<sup>4</sup>*ICT, Departamento de Geociências, Universidade de Évora, 7001-554 Évora, Portugal*

*\* Corresponding author at: Departamento de Geodinámica, Estratigrafía y Paleontología. Facultad de Geología, Universidad Complutense de Madrid, C/ José Antonio Novais, no 2, 28040 Madrid, Spain. Tel.: +34 913944864; fax: +34 913944631*

*E-mail address: rudiez@ucm.es (R. Díez Fernández, corresponding author)*

This article has been accepted for publication and undergone full peer review but has not been through the copyediting, typesetting, pagination and proofreading process which may lead to differences between this version and the Version of Record. Please cite this article as doi: 10.1029/2018TC005224

## Key Points:

- The Calzadilla Ophiolite is a fore-arc ensemble obducted onto a section of a peri-Gondwanan arc in latest Ediacaran times
- Ophiolite obduction was directed to the ESE (present-day coordinates), following a vector directed to mainland Gondwana
- Obduction preceded back-arc and fore-arc spreading in peri-Gondwana, and was followed by the onset of extensional domes and rifting

## Abstract

The Calzadilla Ophiolite is an ensemble of mafic and ultramafic rocks that represents the transition between lower crust and upper mantle of a Cadomian (peri-Gondwanan) fore-arc. Mapping and structural analysis of the ophiolite demonstrates it was obducted in latest Ediacaran times, because the Ediacaran – Early Cambrian sedimentary series (Malcocinado Formation) discordantly covers it. The ophiolite and emplacement-related structures are affected by Variscan deformation (Devonian - Carboniferous), which includes SW-verging overturned folds (D<sub>1</sub>) and thrusts (D<sub>2</sub>), upright folds (D<sub>3</sub>), extensional faults (D<sub>4</sub>), and later faults (D<sub>5</sub>). These phases of deformation are explained in the context of Variscan tectonics as the result of the progressive collision between Gondwana and Laurussia. Qualitative unstraining of Variscan deformation reveals the primary geometry of Ediacaran – Cambrian structures, and uncovers the generation of E-verging thrusts as responsible for the primary obduction of the Calzadilla Ophiolite. Restoration of planar and linear structures associated with this event indicates an Ediacaran, east-directed obduction of the ophiolite, i.e. emplacement of the Cadomian fore-arc onto inner sections of the northern margin of Gondwana. According to regional data, the obduction separates two extension-dominated

stages in the tectonic evolution of the African margin of northern Gondwana preserved in southern Europe. Pre-obduction extension brought about the onset and widening of fore-arc and back-arc basins in the external part of the continent, while post-obduction extension facilitated the formation of extensional migmatitic domes, an oceanward migration of back-arc spreading centers across peri-Gondwana, and the eventual opening of a major basin such as the Rheic Ocean.

**Keywords:** Obduction, Ophiolite, Mantle exhumation, Cadomian Orogen, Variscan Orogen, Iberian Massif

## 1. Introduction

Ophiolite obduction is a common process in subduction-related orogens [Dewey, 1976; Wakabayashi and Dilek, 2003; Edwards *et al.*, 2015]. Examples of ophiolite obduction in the peripheral domains of the northern margin of Precambrian Gondwana include the case of the Bou Azzer Ophiolite in the Anti-Atlas of Morocco [El Hadi *et al.*, 2010], the Frolosh Ophiolite in Kraishte zone, Bulgaria [Kounov *et al.*, 2012], and the Calzadilla Ophiolite in SW Iberia [Arenas *et al.*, 2018]. The reference age for the protoliths and emplacement of these ophiolites is Ediacaran, and the subduction-related activity (magmatism and crustal growth) reported for the sections of African Gondwana preserved along the basement of southern and central Europe strongly suggests that tectonic activity related to subduction under Gondwana extended at least all through the Ediacaran [e.g., D'Lemos *et al.*, 1990; Chantraine *et al.*, 2001; Linnemann *et al.*, 2007].

Orogens resulting from continent-continent collisions are also characterized by significant crustal thickening at the boundaries of colliding plates. Interference between

structures generated in the context of a subduction-related orogen and those formed during continent-continent collision is a very likely option, because the eventual collision and amalgamation of continental landmasses requires previous subduction, either intra-oceanic or sub-continental.

The Variscan orogen (Fig. 1) resulted from the progressive collision between Gondwana and Laurussia during the Devonian and Carboniferous [Matte, 1991]. This collision followed Precambrian and lower Paleozoic tectonic events related to the evolution of the African section of the northern margin of Gondwana. The Precambrian events are generally attributed to the Cadomian Orogeny, which occurred along the northern margin of Gondwana due to collision/accretion processes related to subduction and the dynamics of a continental island arc system [D'Lemos *et al.*, 1990; Strachan and Taylor, 1990; Quesada *et al.*, 1991; Fernández-Suárez *et al.*, 1998; Eguíluz *et al.*, 2000; Ballèvre *et al.*, 2001; Linnemann *et al.*, 2007]. The lower Paleozoic events are thought to be linked to the opening of the Rheic Ocean *s.l.* [Crowley *et al.*, 2000; Murphy *et al.*, 2006; Nance *et al.*, 2010; Díez Fernández *et al.*, 2012].

Exposed ophiolites and high-P metamorphic belts are the best sites to discuss the geometry, structural evolution, kinematics and geodynamic setting of suture zones. Despite how good the inferences about Ediacaran suture zones are in other parts of the Cadomian Orogen (when ophiolites or high-P belts are not exposed), two ophiolites [Kounov *et al.*, 2012; Arenas *et al.*, 2018] are the only indisputable, direct evidence we have on Cadomian suture zones in Europe. One of particular interest is the Calzadilla ophiolite, in SW Iberia (Fig. 2). This ophiolite is discordantly covered by younger Ediacaran – Early Cambrian sedimentary series with regional extent, and the region is affected by contrasting magmatic and thermal events that need a plate-scale approach to be explained (*e.g.*, subduction-related processes). Therefore, the surrounding area of the Calzadilla ophiolite is an almost unique

site to present an integrated view about the dynamics of suturing processes taking place during the Cadomian Orogeny, their consequences, and subsequent evolution.

Given the superimposition of Variscan onto Cadomian deformation in SW Iberia, here we present a structural analysis of the Calzadilla Ophiolite and its surrounding area in order to constrain its structural evolution, emplacement mechanisms and kinematics, as well as the timing and geodynamics associated with each of the pre-Mesozoic orogenic cycles that affected this Ediacaran ophiolite. Since the obduction of this ophiolite took place in latest Ediacaran times, the results presented in this work are used to further a discussion on the evolving geodynamic setting during the Ediacaran – Cambrian transition in southern Europe, a period of major changes in northern Gondwana that can be explained by changeable parameters in a long-lived subduction-related orogen.

## **2. Geological setting**

The Iberian Massif is the southernmost section of the Variscan Orogen (Fig. 1). The Iberian section of Gondwana was influenced by long-lived subduction during the Precambrian [*Bandrés et al.*, 2004; *Pereira et al.*, 2006; *Linnemann et al.*, 2008; *Díez Fernández et al.*, 2010; *Albert et al.*, 2015b; *Henriques et al.*, 2015; *Rubio-Ordóñez et al.*, 2015]. Whole-rock geochemistry and isotopic analysis of both sedimentary and igneous rocks ranging c. 600 Ma and c. 525 Ma in age are compatible with an arc-related setting [*Bandrés et al.*, 2004; *Fuenlabrada et al.*, 2012, 2016; *Henriques et al.*, 2015; *Sánchez-García et al.*, 2014; *Sánchez Lorda et al.*, 2014; *Díez Fernández et al.*, 2017]. Pre-Variscan deformation within that age range has been thus attributed (*s.l.*) to the dynamics of an arc-trench system [*Quesada*, 1990; *Eguíluz et al.*, 2000]. Most authors agree that Precambrian subduction gave way to a complex continental arc system rimming Gondwana from at least 650 Ma ago, although the isotopic record preserved in detrital grains extracted from younger sedimentary

basins suggests an older age for the onset of subduction (~750-650 Ma; *Albert et al.*, 2015a; *Pereira*, 2015, and references therein). Similar conclusions have been put forward for other sections of the Variscan Orogen of western Europe [*Brown et al.*, 1990; *D'Lemos et al.*, 1990; *Chantraine et al.*, 2001; *Linnemann et al.*, 2007].

The Cambrian was a time of changes and different record for the basins of the Iberian Massif. Extension and rift-related magmatism seem to dominate in the Cambrian and Ordovician basins preserved in SW Iberia (Ossa-Morena Complex in Figure 2) [*Chichorro et al.*, 2008; *Pereira et al.*, 2012b; *Sánchez-García et al.*, 2010; *Díez Fernández et al.*, 2015], whereas various combinations of arc-related magmatism, extension, and rift-related magmatism are observed in Central Iberia [*Montero et al.*, 2007; *Castro et al.*, 2009; *Rubio-Ordóñez et al.*, 2012; *García-Arias et al.*, 2018] and in NW Iberia [*Abati et al.*, 2010; *Andonaegui et al.*, 2017; *Díez Fernández et al.*, 2012].

The Ediacaran–Cambrian geodynamic evolution is well-recorded in SW Iberia (Ossa-Morena Complex in Figures 2 and 3). The Ediacaran series, referred to as the Série Negra [*Alia*, 1963; *Carvalhosa*, 1965; *Gonçalves*, 1971], are interpreted as derived from the erosion and coeval magmatic activity in the context of a peri-Gondwanan continental arc [*Pereira et al.*, 2006, 2012b; *Linnemann et al.*, 2008; *Díez Fernández et al.*, 2017]. Its fore-arc section is represented by the sequences located to the SW, whereas the intra-arc sections are located more to the N and NE (present-day coordinates), thus suggesting NE subduction polarity (beneath Gondwana) in Ediacaran times [*Sánchez Lorda et al.*, 2014, 2016; *Arenas et al.*, 2018]. Cambrian strata lie discordantly over these series [*Gonçalves*, 1971; *Liñán et al.*, 1984; *Eguíluz*, 1987; *Quesada*, 1990; *Pereira et al.*, 2006] and are interbedded with progressively more alkaline igneous rocks [*Sánchez-García et al.*, 2010]. Both Precambrian and Paleozoic rocks are affected by complex Variscan deformation and metamorphism [*Simancas et al.*, 2003; *Silva and Pereira*, 2004; *Díaz Azpiroz et al.*, 2006; *Ribeiro et al.*,

2007]. In this regard, the recognition of Precambrian and Cambrian (Cadomian) deformation is clear in some places [e.g., *Quesada*, 1990; *Eguíluz and Abalos*, 1992; *Pereira et al.*, 2006; *Sánchez-García et al.*, 2010], but quite disputed in other areas [*Abalos et al.*, 1991; *Azor et al.*, 1993].

## 2.1 Lithostratigraphy of the study area

Mapping of the lithostratigraphic units is presented in Figure 4a. A collection of pictures showing relevant observations is provided as Supplementary Material (SM-1x).

The study area includes three massifs of metaultramafic rocks and minor metagabbros [*Fernández-Carrasco et al.*, 1980; *Arriola et al.*, 1984; *Monterrubio*, 1991; *Jiménez-Díaz*, 2008]. The metaultramafic rocks are variably serpentinitized harzburgites and dunites, enveloping veins of clinopyroxenite and Al-rich podiform chromitite bodies [*Arriola et al.*, 1984; *Aguayo Fernández*, 1985; *Martos et al.*, 2010; *Merinero et al.*, 2013]. This ensemble is considered to represent the mantle-crust transition zone (Moho) in ophiolites of MORB or supra-subduction zone types [*Pearce et al.*, 1984a], and so the metamorphosed ultramafic-mafic massifs of the study area have been considered as ophiolitic bodies [*Martos et al.*, 2010; *Merinero et al.*, 2013]. In a recent work, this ensemble was referred to as the Calzadilla Ophiolite [*Díez Fernández and Arenas*, 2015]. Lenses of serpentinite are also found within one of the metasedimentary rock sequences (Serie Negra Group) that crops out nearby one of the metaultramafic massifs. The correlation of these lenses with the rest of the metaultramafics will be discussed below. U-Pb dating of magmatic zircon extracted from the metagabbros (amphibolites) of the Calzadilla Ophiolite has yielded a crystallization age of ca. 600 Ma for the protolith, whereas its whole-rock major and trace element composition suggests a fore-arc setting for its development [*Arenas et al.*, 2018].

The Serie Negra Group represents the oldest series so far described in SW Iberia, which has been divided into the Montemolín and Tentudía formations. In the study area, the Montemolín Formation constitutes the lower part of the Serie Negra Group [Quesada, 1991]. It consists of quartz-rich metasediments, graphite-rich mica schists, black quartzites and minor marbles, all of which are intercalated with metabasites (more abundant to the top of the sequence, Montemolín amphibolites; Eguíluz, 1987). This formation is intruded by the  $552 \pm 2$  Ma old Ahillones pluton [Ordóñez Casado, 1998], and has a maximum depositional age of  $591 \pm 11$  Ma (U-Pb in detrital zircon; Ordóñez Casado et al., 2009), although a protolith crystallization age of  $\sim 600$  Ma has been obtained in some metabasites (U-Pb in magmatic zircon; Schäfer, 1990).

The upper part of the Serie Negra Group is referred to as the Tentudía Formation and includes progressively thicker metagreywacke beds that alternate with slates and rare felsic metaigneous rocks and metabasites. The maximum depositional age of this formation is constrained to c. 560-550 Ma (U-Pb in detrital zircon; Schäfer et al., 1993; Ordóñez Casado, 1998; Fernández-Suárez et al., 2002), slightly older than the maximum depositional age of c. 545-544 Ma obtained for other exposures of the Serie Negra Group [Linnemann et al., 2008].

The Malcocinado Formation [Fricke, 1941] rests discordant over all of the previously described lithologies. It consists of slates, metasediments (arkoses) and metaconglomerates that are interbedded with metaandesites (andesitic tuffs) and rare metadiorites, metadiabases, and metacinerites. The metaconglomerates show gravel to (less frequent) boulder sized clasts of andesite, granitoid, porphyroid, slate, metagreywacke, hydrothermal quartz and black quartzite (SM-1a). The metaandesites of the Malcocinado Formation and correlatives (San Jerónimo Formation; Liñán et al., 1984) show calc-alkaline geochemistry [Sánchez-Carretero et al., 1989] and strongly radiogenic Nd isotope signature [Pin et al., 2002].

The maximum depositional age of some parts of the Malcocinado Formation is roughly constrained to  $522 \pm 8$  Ma (U-Pb in a single detrital zircon; *Ordóñez-Casado et al.*, 1998), and its minimum age does not really differ (within error) from that number, as the lowermost overlying sedimentary succession that covers this series has been attributed to Early Cambrian (fossils and detrital zircon in Torreárboles Formation and correlatives; *Liñán et al.*, 1984; *Linnemann et al.*, 2008). Further considerations on the age of this series are the presence of late Ediacaran trace fossils [*Liñán*, 1978] and microfossils [*Liñán and Palacios*, 1983; *Palacios*, 1989]. Collectively, all these data suggest a late Ediacaran to lowermost Cambrian age for the Malcocinado Formation.

The Torreárboles Formation lies also discordant over all the previous formations. It is a succession of metasandstones (mostly arkoses) and some metaconglomerates that includes progressively more abundant slate beds to the top [*Liñán et al.*, 1993]. The age of this series, based on fossil content, is Early Cambrian [*Liñán and Palacios*, 1983; *Liñán*, 1984; *Liñán et al.*, 1984].

The Zafra Formation overlies conformably the Torreárboles Formation. It includes slates and thin bedded (cm to m scale) marbles, which are more abundant to the top. Its stratigraphic position and the age of overlying and underlying sequences (see below) suggest an Early Cambrian age [*Liñán and Quesada*, 1990].

In the study area, the Loma del Aire Formation [*Garrot*, 1976] is made of slates, with some minor metasandstones, metatuffs and sills. Lithostratigraphical complexity of this formation increases to the west, including marbles, and a Cambrian crystallization age (c. 526-505 Ma) has been obtained for some of its metaigneous rocks (U-Pb magmatic zircon dating; *Sánchez-García et al.*, 2016).

### 3. Structure

Figures 4a and 5a are two geological maps of the study area showing the attitude of planar and linear structures, respectively. Reference points (RP-X) shown in Figure 5a will be used for locating relevant sites during data presentation.

A limited Cenozoic sedimentary cover allows observing a complex crystalline basement consisting of Precambrian and lower Paleozoic rocks. Markedly curved and sinuous contacts between formations described in section 2 are truncated by straighter fault traces to make a regional structure defined by folds and normal, reverse or strike-slip faults (Fig. 6). Two paired kilometer-scale folds, the Atarja anticline (RP-1-3) and the Fuente de Cantos syncline (RP-4-6), and numerous minor folds affect the whole basement rocks (Fig. 5a). Other relatively major folds of the region (e.g., RP-7 and -8; Fig. 5a) represent culmination folds related to the Atarja anticline (Fig. 6b).

Seven main faults exist in the study area (Fig. 5a): (i) Los Llanos thrust (RP-3 and -9), (ii) Moralejo normal fault (RP-10-11), (iii) Lobo normal fault (RP-12), (iv) Cerro Cabrera thrust imbricates (RP-13-16), (v) El Villar thrust imbricates (RP-17), (vi) Gordillo thrust (RP-18), and (vii) Moro thrust (RP-19).

Two regional unconformities have been mapped. Both of them are frequently marked by conglomerates at the base. In map view these unconformities are revealed by the oblique and cross-cutting nature of their basal contacts relative to underlying series (RP-2 and -20; Fig. 5a). The angular unconformity between the Malcocinado Formation and Serie Negra Group (e.g. RP-20; Fig. 5a) makes evident a Cadomian (Precambrian) deformation phase, whereas the angular unconformity between Torreárboles Formation and all older formations accounts for Cambrian deformation. Both of them are pre-Variscan *sensu stricto*. The rest of phases of deformation that affect the Precambrian and lower Paleozoic rocks are Variscan (see below). Aiming at unifying nomenclature, Precambrian and Cambrian (pre-Variscan)

phases of deformation will be referred to as  $pcD_1$ ,  $pcD_2$ , etc., consecutively. The sequence of Variscan deformations will be described adhering to the classical scheme, and each phase will be thus named  $D_1$ ,  $D_2$ ,  $D_3$ , etc., consecutively.

Seven main phases of deformation can be identified in the study area: one is Precambrian and is associated with penetrative foliation ( $pcD_1$ ;  $S_{pcD1}$ ), one is Cambrian and has no foliation ( $pcD_2$ ), and up to five are Variscan ( $D_1$ - $D_5$ ;  $S_1$ - $S_5$ ).  $D_1$  is associated with SW-verging overturned folds and penetrative axial plane foliation ( $S_1$ ).  $S_1$  is actually the second foliation that affects the Serie Negra Group, but represents the first foliation for the Malcocinado Formation and for younger Paleozoic series.  $D_2$  is represented by SW-verging thrusts, while  $D_3$  produced upright folds and local axial plane foliation ( $S_3$ ). Moderate-angle extensional faults formed during  $D_4$ , and a set of late, E-W to NE-SW-trending high-angle faults is the latest main deformation ( $D_5$ ) observed in the study area. A set of E-W-trending and very open folds are also observed (SM-1b). These folds affect  $S_1$ , but no crosscutting relationship with respect to the other phases of deformation was identified. This deformation event, however, is extremely local and will be treated no further. A possible estimation on the age of Variscan deformation ( $D_1$ - $D_5$ ) can be obtained by comparing the sequence of structures formed in the study area with the age of equivalent phases of deformation dated in nearby sections of SW Iberia. In this regard, the age of  $D_1$  folds and  $D_2$  thrusts is Devonian *s.l.*, whereas the age of subsequent deformation is Bashkirian-Moscovian ( $D_3$ ), and probably Gzhelian and even Permian ( $D_4$ - $D_5$ ) (see extended revision in *Díez Fernández et al.*, 2016).

### 3.1 Geometrical and kinematic analysis of regional structures

#### 3.1.1 Precambrian (Cadomian) deformation ( $pcD_1$ ): El Villar thrust imbricates and $S_{pcD1}$ foliation

The Malcocinado Formation is unconformably overlying the previously deformed Calzadilla Ophiolite and Serie Negra Group (RP-20; Fig. 5a), like in other sections of SW Iberia [e.g., *Quesada*, 1990]. The discordant character of this contact can be observed north of Calzadilla de los Barros village (SM-1c). Additionally, pebbles of deformed black quartzite can be found in metaconglomerates of the Malcocinado Formation (SM-1a; note those quartzites are exclusive to the Ediacaran Serie Negra). No Serie Negra Group lithologies, but just the Calzadilla Ophiolite alone, crops out to the northeastern half of the study area and under Malcocinado Formation. This suggests wedging of the Serie Negra Group to the northeast under Malcocinado Formation (Fig. 4a), as directly observed at RP-20 (Fig. 5a). Therefore, when the Malcocinado Formation was deposited, the contact between the Calzadilla Ophiolite and Serie Negra Group dipped to the southwest (Fig. 6).

Tectonic slices of serpentinite (after harzburgite and dunite; *Jiménez-Díaz et al.*, 2009) occur exclusively within the Montemolín Formation (RP-17; Fig. 5a). These lenses of upper mantle rocks range in thickness between tens and several hundred meters, and their bases have been put in contact with the metasedimentary rocks of Montemolín Formation via thrusting. Accordingly, this particular set of lenses is referred to as El Villar thrust imbricates. Although both the upper and lower contact of the serpentinite lenses may be thrusts, we should not discard the hypothesis that one of the contacts is a thrust and the other one could be either a sedimentary (nonconformity?) contact and/or an extensional fault. Poor-quality and rather limited outcropping did not allow testing these two possibilities. Despite Variscan thrust imbricates developed in the study area (see section 3.1.4), El Villar thrusts are

Ediacaran or Cambrian in age, since the Torreárboles Formation unconformably overlies some of the contacts of the serpentinite lenses (RP-21; Fig. 5a).

Intense strain characterizes the section of the Serie Negra Group that crops out west of Calzadilla de los Barros village and around El Villar thrust imbricates (RP-2, -11, -13, -16, -17; Fig. 5a). Bedding in the metasedimentary rocks is deeply obliterated and a mylonitic (banding) foliation dominates this entire occurrence. Such foliation can be observed in the schists and black quartzites (SM-1d) of the Serie Negra Group, as well as in the amphibolites (SM-1e) of the Calzadilla Ophiolite. This type of foliation is absent in the rest of the overlying sedimentary successions (Malcocinado, Torreárboles formations, etc.), which exhibit significantly lower finite strain at regional scale and its main (usually single) foliation is an axial plane cleavage (see section 3.1.3). The mylonitic banding is the first foliation observed in this section of the Serie Negra Group ( $S_{pcD1}$ ). Tectonic foliations in other parts of the Serie Negra Group show a comparable relationship with the overlying successions in the study area. However, finite strain in those other parts (e.g. Tentudía Formation) is much lower compared to the outcrops west of Calzadilla de los Barros village, thus indicating regional heterogeneities of strain related to the development of  $S_{pcD1}$ .  $S_{pcD1}$  shows mineral and stretching lineation ( $L_{S_{pcD1}}$ ), whose trend varies from NW-SE to E-W (Fig. 5e), and with plunge directions both to the E and W. In ultramafic rocks of the Calzadilla Ophiolite, the mineral lineation is defined by serpentine fibers, whereas the stretching lineation is marked by stretched pyroxene crystals (SM-1f). In the amphibolites, the mineral lineation is defined by amphibole porphyroblasts (SM-1e), and the stretching lineation by the superimposed stretching of some of those porphyroblasts (SM-1r). In the metasedimentary rocks of the Serie Negra Group, the mineral lineation is marked by recrystallized quartz and mica, while the stretching lineation is defined by stretched quartz segregates (SM-1d) and rock fragments

in metagreywackes (SM-1g). Kinematic indicators associated with this fabric will be described in a later section.

The age of Precambrian deformation ( $pcD_1$ ) can be constrained between the age of the basal contact of the Malcocinado Formation (latest Ediacaran; see section 2.1) and the age of the youngest strata of Serie Negra Group (Tentudía Formation), i.e. latest Ediacaran (maximum depositional age of ~550-540 Ma).

### 3.1.2 Cambrian deformation ( $pcD_2$ )

The Torreárboles Formation lies discordant upon both Malcocinado Formation and Serie Negra Group (RP-2; Fig. 5a). As a result, the Malcocinado Formation wedges to the west (RP-2 and -22; Fig. 5a), thus indicating east-directed tilting of the pre-Torreárboles Formation record. The thickness of the Malcocinado Formation also increases significantly to the NE, so a component of rotation towards NE must be considered. No penetrative or local tectonic fabrics have been identified that could be ascribed to this phase of deformation, and the tilting cannot be yet attributed to the movement of any particular fault of the study area. A reference age for the Cambrian deformation ( $pcD_2$ ) may be the age of the youngest strata in the Torreárboles Formation itself, which is in turn constrained by the age of the oldest strata of the overlying Zafra Formation, i.e. c. 542-526 Ma (Early Cambrian; see section 2.1).

### 3.1.3 $D_1$ Variscan deformation: SW-verging overturned folds

The Precambrian and lower Paleozoic rocks are deformed into a pair of major SW-verging overturned folds ( $D_1$ ; Fig. 6; SM-1h). Fold traces of these folds trend NW-SE (Fig. 4a), roughly parallel to their fold axes (Figs. 4b, 4c, 5b). A widespread, NW-SE trending foliation affects all of the Precambrian and lower Paleozoic lithologies of the study area (SM-1i), being the first tectonic fabric for the Malcocinado and younger formations ( $S_1$ ). In

general terms,  $S_1$  is a slaty cleavage, but it may also appear as a spaced cleavage in the serpentinites of the Calzadilla Ophiolite (SM-1j).  $S_1$  can also occur as a crenulation cleavage (with associated crenulation lineation;  $Lb_1$ ) in the Serie Negra Group (SM-1k), or as a rough or stylolitic cleavage in younger coarse-grained metasandstones and marbles, respectively. No significant strain gradient has been identified.  $S_1$  shows mineral ( $Lm_1$ ) and stretching ( $Ls_1$ ) lineation trending NW-SE (Fig. 5c), with dominant plunge to the NW. The mineral lineation is defined by micas, whereas the long axis of stretched pebbles in conglomerates marks the attitude of the stretching lineation (SM-1l).

$S_1$  trends nearly parallel to either bedding or Precambrian foliation ( $S_{pcD1}$ ) along the limbs of overturned folds, but its trend is highly oblique to perpendicular over the hinge zone of those folds. However,  $S_1$  is always oblique to either  $S_0$  or  $S_{pcD1}$ , and field observations of their angular relationship has allowed distinguishing normal and reverse limbs of folds associated with axial plane  $S_1$  (Fig. 6).  $S_1$  dips dominantly to the NE (Fig. 4d), as expected for an axial plane foliation related to SW-verging folds. But  $S_1$  may also be vertical or dips to the SW, without being accompanied by a change in the dip direction of bedding, thus suggesting mesoscale cleavage refraction associated with  $D_1$  folding.

$D_1$  fold axes plunge regionally to the NW, as indicated by direct observation of micro- to mesofolds (SM-1h, -1m; Fig. 5b),  $S_0$ - $S_1$  intersection lineations (Fig. 5b), or by  $\pi$ -diagrams constructed from measurements of bedding (Fig. 4b),  $S_{pcD1}$  (Fig. 4c), and  $S_1$  (Fig. 4d). Local variations in plunge direction of  $D_1$  folds do exist, as observed in stereographic plots. All those changes in plunge occur in zones affected by later upright folding ( $D_3$ ), whose folds are characterized by such changes too (see below). However, closures of major folds point out the NW-plunging character of  $D_1$  folds at a large scale, thus exposing younger successions to the NW and older ones to the SE (Fig. 4a).

### 3.1.4 $D_2$ Variscan deformation: thrusts

$D_1$  folds are cut by high- to moderate-angle reverse faults (SW-verging thrusts; SM-1n). Previous stratigraphy and structure can be followed through each block of these thrusts within the study area, so no great offsets are implied for any of them. Almost all of the thrusts occur entirely or mostly along the reverse limb of  $D_1$  folds. These faults can be grouped in two sets according to their structural relationships and/or cartographic connection: one set of one fault in the north (RP-18; Gordillo thrust; Fig. 5a), and other set of five faults located to the west and south of Calzadilla de los Barros village (Los Llanos thrust, Cerro Cabrera thrust imbricates, and Moro thrust; RP-3, -9, -13, -14, -15, -16, -19; Fig. 5a), which from now on will be collectively referred to as Los Llanos thrust system.

No cartographic connection was found between the two aforementioned fault sets.

Faults of the Los Llanos thrust system connect with each other (as deduced from their mapping), with the exception of the two exposures of the Los Llanos thrust (RP-3 and -9; separated by a later fault) and the Moro thrust (RP-19) (Fig. 5a). Los Llanos thrust system constitutes a set of imbricated faults, for which the Los Llanos thrust is the sole fault. The lower thrust of the Cerro Cabrera thrust imbricates (RP-13 and -16) curves to join the sole thrust (RP-23) (Fig. 5a). To the southwest, rejoining of that lower thrust of Cerro Cabrera with the sole thrust is obliterated (but assumed) by a later fault (RP-11; Fig. 5a). Therefore the exposure of Precambrian and Cambrian successions west and southwest of Calzadilla de los Barros village is regarded as a horse formed in a thrust imbricate fan with a rejoining splay. Two thrusts (RP-14-15) branch off upwards from the lower thrust of Cerro Cabrera to define another system of imbricate thrust faults. The Moro thrust could be regarded as a back-thrust relative to the Los Llanos fault system, the exposure of the main body of metaultramafics in the study area occupying the core of a pop-up structure.

Planar ( $S_2$ ) and linear kinematic indicators were observed in relation to these thrusts, although limited outcropping has only allowed a preliminary kinematic approach. Microstructural features of planar fabrics will be described in section 3.2.  $S_2$  is parallel to fault surfaces, and dip values range between  $35^\circ$  and  $65^\circ$ . In the Los Llanos thrust, a component of left-lateral movement is inferred from C'-S and C-S structures (SM-1o). This component can also be inferred from mapping. Linear fabrics include fault striae and slickenfibers of quartz or calcite (SM-1p), from which a left-lateral movement is also inferred (linear fabrics are gently to moderate E-plunging in NE-dipping fault surfaces).

### 3.1.5 $D_3$ Variscan deformation: upright folds

$S_{pcD1}$  and  $S_1$  can be locally affected by upright folds (SM-1q). Although no cross-cutting relationships have been observed with  $S_2$  in the study area, observations made in adjacent areas indicate that these upright folds formed after  $D_2$  thrusts [Expósito Ramos, 2005]. These folds may develop subvertical crenulation cleavage ( $S_3$ ), with a mean strike of NW-SE, but dip-direction may be either to the NE or SW (Fig. 4e). Associated crenulation lineation ( $Lb_3$ ) trends NW-SE, and its plunge can be to the NW, horizontal, or to the SE (Fig. 5d).  $D_3$  fold axes (Fig. 5d) are less dispersed in trend than  $D_1$  fold axes (Fig. 5b), as expected for a superimposition of two oblique fold systems, both relative to their trend and their plunge direction. However, the regional trend of fold axes and their traces seem similar for both fold systems, so obliquity must be quite limited. The distribution of these folds and associated fabrics is not random as they occur almost exclusively east of the Moralejo normal fault (RP-10-11; Fig. 5a), i.e. in its upper block.

### 3.1.6 $D_4$ Variscan deformation: normal faults

$D_1$  folds,  $D_2$  thrusts and  $D_3$  folds are cut by moderate-angle normal faults ( $D_4$ ). Their fault traces trend NW-SE (Fig. 4a) and fault planes dip to the NE (Fig. 6b). No good quality exposures were found as to constrain lateral movement along these faults, or to characterize planar or linear tectonic fabrics related to their development. Offsets, however, are probably moderate (few kilometers at most), since no major disruption of previous structures or metamorphic zoning are associated with their movement.

Two main  $D_4$  extensional faults were identified. In the southwestern part, the Lobo normal fault cuts the hinge zone of a  $D_1$  synform, and puts in contact the Malcocinado and Loma del Aire formations, subtracting part of the stratigraphy because the Torreárboles and Zafra formations are missing (RP-12; Fig. 5a). In the central (RP-11) and southern part of the study area (RP-10), the Moralejo normal fault cuts  $D_1$  and  $D_3$  folds and a section of Los Llanos thrust (Fig. 5a). The tip of the Moralejo normal fault is located to the north, where the fault trace seems unaffected by local  $D_3$  folds, which are probably cut by it. The Moralejo normal fault shows a rejoining splay defining a single horse southeast of Fuente de Cantos village (RP-24; Fig. 5a).

### 3.1.7 $D_5$ Variscan deformation: subvertical faults

All of the previous structures are cut by two sets of subvertical faults. One set trends NE-SW and the other one trends E-W. Offsets are quite limited, and barely surpass a few hundred meters for the major faults. No relevant topographic changes are associated with any of them. Their age is assumed to be Variscan, since other late faults with similar geometry are covered by post-Variscan strata (Fig. 4a).

### 3.2 Microstructural, isotopic age and metamorphic approach

The first foliation found in the metapelites of the Montemolín Formation that occurs west of Calzadilla de los Barros village ( $S_{pcD1}$ ) is defined by oriented quartz, white mica, brown-green biotite, plagioclase, and opaques, whereas in the rest of the metapelites of this Ediacaran series  $S_{pcD1}$  includes quartz, white mica, brown-red biotite, plagioclase, and opaques [Fernández-Carrasco *et al.*, 1980]. The first foliation ( $S_{pcD1}$ ) of the metabasites in the southeastern part of the Montemolín Formation is marked by plagioclase, amphibole, epidote, titanite, and minor biotite (SM-1r). The first foliation ( $S_{pcD1}$ ) recognized in the metapelites of the Tentudía Formation is defined by oriented quartz, white mica, green-brown biotite, plagioclase, chlorite and opaques in the upper parts of the series (SM-1s), whereas in the lower parts biotite becomes brown and brown-red suggesting an increase in the metamorphism temperature.  $S_{pcD1}$  has been dated at late Ediacaran [c. 550-560 Ma; Ar-Ar dating; Blatrix and Burg, 1981; Dallmeyer and Quesada, 1992].

The first foliation in the metapelites of the Malcocinado Formation and younger formations of the study area ( $S_1$ ) consists of quartz, white mica, plagioclase, green-brown biotite, sericite and chlorite (SM-1t).  $S_1$  has been dated at Devonian [400-385 Ma; K-Ar and Ar/Ar dating; Galindo *et al.*, 1986, 1987; Dallmeyer and Quesada, 1992]. The second foliation in the metapelites of the Serie Negra Group shows a similar mineral association, is observed as a crenulation cleavage superimposed on  $S_{pcD1}$  (SM-1k), is geometrically and structurally equivalent to  $S_1$ , and has yielded isotopic ages coeval with  $S_1$  [Dallmeyer and Quesada, 1992]. Consequently, two separate metamorphic cycles (Cadomian and Variscan) developed in the study area, since the (metamorphosed) Malcocinado Formation rests discordantly onto a (previously metamorphosed) Serie Negra Group.

The serpentinites of the Calzadilla Ophiolite show (at least) three different foliations (see extended petrographic description by *Arriola et al.*, 1984; *Jiménez-Díaz*, 2008; *Jiménez-Díaz et al.*, 2009). The first foliation is widespread, partly cataclastic, and contains numerous asymmetric structures (C'-type slip zones, S-C-like fabrics, and mica-fish-like structures) suggesting a component of simple shear (SM-1u) (shear sense will be presented below). According to the sequence of fabric development in the region, this fabric correlates well with  $S_{pcD1}$  (note this foliation is affected by  $D_1$  folds; Fig. 4a). Minerals defining the non-cataclastic component of the fabric are serpentine, talc, chlorite, and carbonates, and primary phases of the peridotitic protolith such as pyroxene, chromite, and magnetite are re-oriented to the fabric in the sections dominated by cataclastic processes. Locally, some metapyroxenites show a foliation defined by tremolite, chlorite, epidote, and carbonates. The second foliation is not as penetrative as the first one (SM-1j, and -1v), and is regionally parallel to  $S_1$  and assumed to be an equivalent crenulation cleavage (SM-1v). Cataclasis associated with the second fabric is almost absent, and minerals defining this foliation are mostly serpentine and reoriented pyroxene. At a local scale, the metamorphosed peridotites present a third, discrete cataclastic foliation defined by talc and carbonate, and minor amounts of magnetite, serpentine and chlorite, although the latter can be also the dominant phase in some cases. This third fabric is observed in the damage zones related to Variscan thrusts ( $S_2$ ).

The amphibolites of the Calzadilla Ophiolite show two foliations. The first one is penetrative and roughly parallel to the first one observed in adjacent serpentinites ( $S_{pcD1}$ ). It is defined by hornblende, plagioclase, titanite, and epidote. U-Pb dating of zircon grains from metagabbros of the Calzadilla Ophiolite revealed a possible post-protolith (re-?) crystallization event at  $c. 539 \pm 13$  Ma [*Arenas et al.*, 2018], which matches, within error, with the age interval considered for  $pcD_1$ . The second foliation is spaced, defined by

actinolite-tremolite, chlorite, plagioclase, and epidote (SM-1e), and correlates with  $S_1$ .

Amphibolites with more penetrative  $S_1$  are characterized by finer grain size hornblende and plagioclase.

$S_2$  developed in metapelites consists of a set of anastomosing foliation and shear bands cutting across previous foliation (SM-1w). Shear bands are filled with recrystallized quartz, mica, opaques, and may contain carbonates, whereas the foliation consists of reoriented mineral from previous fabrics and newly-formed quartz, mica and sericite.

Previous foliation near  $S_2$  is affected by crenulation and variably intense sericitization.

According to mineral parageneses,  $pcD_1$  (Cadomian) metamorphism is dominantly low-grade, but in the case of the metabasites of the Calzadilla Ophiolite and in the lower amphibolites of the Montemolín Formation the grade seems slightly higher than in the rest of surrounding metapelitic rocks of Montemolín and Tentudía formations. Therefore, two juxtaposed, normally-zoned metamorphic domains emerge within the Ediacaran rocks exhibiting  $S_{pcD_1}$ . On the one hand, there would be a normal gradation from the (hotter; amphibolite facies) metabasites of the Calzadilla Ophiolite to the (colder; greenschists facies) metapelites of the Serie Negra Group located next to the SW (note that this gradient is currently inverted by the reverse limb of the Atarja anticline). Similarly, a normal gradient exists within the Serie Negra Group that appears to the south, which ranges from greenschists facies in the upper part of the Tentudía Formation to amphibolite facies conditions within the Montemolín Formation. This double zonation will be explained in the light of major Cadomian structures discussed below. Finally,  $D_1$ - $D_5$  (Variscan) metamorphism is low-grade, developed under greenschists facies conditions, and shows no clear metamorphic gradients.

Kinematic criteria in  $S_{pcD_1}$ , including sigma, C-S, C'-S, and mica-fish-like structures in the Serie Negra Group (SM-1x) and in the Calzadilla Ophiolite (SM-1u), consistently indicate top-to-the-E or -SE sense of shear. No clear asymmetric fabrics were observed in  $S_1$ ,

but we cannot rule out the possibility that the vergence of major  $D_1$  folds (Fig. 6) and regional attitude of  $S_1$  (Fig. 4d) are related to a component of top-to-the-SW shearing.  $S_2$  shows SC and C'-S structures with top-to-the-SW kinematics, (SM-1o and -1w), thus supporting a SW-directed simple shear component for this Variscan deformation.

### 3.3 Geometry and kinematics of major Cadomian (Ediacaran) structures

El Villar thrust imbricates occur at the reverse limb of the Atarja-Fuente de Cantos  $D_1$  folds (RP-17, -21). A partial, qualitative reconstruction of the pre-Variscan and pre-Cambrian tilting structure in this area can be obtained from a section made from the extrados to the intrados of the Atarja anticline (see sketch in Fig. 7). If we unfolded this section, we would see that the set of imbricates rest on top of a slice of Serie Negra Group (cropping out between RP-2, -16, -13, and -11), then (below) a package of amphibolites (metagabbros) (RP-20), and finally (below) a massif of metaperidotites (RP-14). The lens-shape geometry of the ultramafic rocks probably corresponds to boudins of larger ultramafic bodies, whose structural continuity was lost to intense stretching within the ductile shear zones that emplaced them to the pre-Variscan structural position they are observed today.

Further positioning of Precambrian outcrops is possible using the geometry of  $D_1$  folds as a guide. The Calzadilla Ophiolite occupied a different structural level in the pre- $D_1$  folding structure relative to the rest of the Serie Negra Group that is located to the S and SE. Given that the plunge of the Atarja anticline is consistently to the NW (Fig. 5a and b), the metaultramafics occupy an extrados position in the Atarja anticline relative to the SE exposure of the Serie Negra Group (Fig. 6a). Therefore, the massif of metaperidotites would rest on top of the Serie Negra Group located to the SE (RP-3) (Fig. 7). Also, the domains affected by amphibolite facies Ediacaran metamorphism observed next to the tectonic slices located to the NW (e.g., amphibolites at RP-20) are on top of a sequence deformed under

greenschist facies conditions (e.g., Tentudía Formation). Similarly, the (older) Montemolín Formation affected by the El Villar thrust imbricates (RP-17) is on top of the (younger) Tentudía Formation that crops out to the SE (RP-3), which is in normal position relative to Montemolín Formation exposures further to the SE (RP-10).

The apparent southwest dip of the contact between the Calzadilla ophiolite and overlying Serie Negra Group in latest Ediacaran times (see section 3.1.1) is a first qualitative approach to the paleo-dip direction of major tectonic contacts recognized in the study area. After undoing  $D_1$  fold rotations in bedding surfaces of the Malcocinado Formation (Fig. 8a), and tracking those rotations in  $S_{pcD1}$  measurements, we have obtained a paleo-orientation of  $S_{pcD1}$  located just below the discordance between Serie Negra Group and the Malcocinado Formation after the Cambrian tilting (Fig. 8b). Data for restoration are included as Supplementary Material (SM-2). An estimation on the primary orientation of  $S_{pcD1}$  is possible by unmaking the Cambrian tilting ( $pcD_2$ ) at each site, and tracking such rotation in  $S_{pcD1}$ . The dominant E-dipping character of  $S_0$  in the Malcocinado Formation before  $D_1$  (Fig. 8a) indicates East-directed Cambrian tilting, as deduced in section 3.1.2. This exercise yields a primary W- to SW-dipping orientation for  $S_{pcD1}$  (Fig. 8c).

Figure 8d includes a plot of Precambrian mineral and stretching lineations along with the sense of shear observed (Fig. 5e), plus the statistically calculated orientation of the axis of  $D_1$  folds (Fig. 4b) and the regional trend of  $D_1$  fold axes extracted from that calculation. Note how the Precambrian lineations define a tail that goes from approximately E-W trends up to the virtual line defined by the regional trend of  $D_1$  folds. This latter line represents the regional trend of a linear fabric attractor [*Passchier, 1997*] towards which the Precambrian lineations have variably rotated from their primary orientation due to superimposed  $D_1$  folding. In this case, the lineation tails indicate a primary E-W trend for the Precambrian lineations and a top-to-the-E sense of shear associated with  $pcD_1$ .

With an inferred W to SW paleo-dip direction of Ediacaran planar structures in the study area, the structural position of the massif of metaperidotites that rests on top of Serie Negra Group located to the SE could be explained by yet another Precambrian thrust, which would occur under the El Villar thrust imbricates (Fig. 7). This thrust explains the juxtaposition of two Cadomian, normally-graded metamorphic series, and is currently cut and hidden by the Malcocinado Formation plus the Moralejo normal fault (RP-11). A combination of W to SW paleo-dip directions for major Precambrian structures with their top-to-the-E kinematics (Fig. 8d) indicates E-directed tectonic transport during Ediacaran thrusting.

#### **4. Discussion**

##### *4.1 Variscan (Devonian - Carboniferous) structures: development and regional integration*

SW-verging folds, equivalent to  $D_1$  folds of the study area, represent the first Variscan deformation preserved in SW Iberia. The asymmetry of the paired  $D_1$  folds studied here is compatible with a normal limb position across a larger  $D_1$  fold such as the Olivenza-Monesterio antiform [Eguíluz, 1987; Eguíluz *et al.*, 1997]. Considering just the southwestern part of the Upper Allochthon of the Ossa-Morena Complex (Fig. 2),  $D_1$  overturned folds affect Ediacaran up to Early Devonian strata. As a whole, that folded succession has been interpreted as the infill of sedimentary basins placed in an outboard position, probably the most external one, across the margin of Gondwana before its collision against Laurussia [Quesada, 2006; Ribeiro *et al.*, 2007; Simancas *et al.*, 2009; Díez Fernández *et al.*, 2016]. The South-Portuguese Zone, widely acknowledged as a Laurussian counterpart [e.g., Braid *et al.*, 2011; Pérez-Cáceres *et al.*, 2017], is located right to the southwest (Fig. 1). Early Variscan deformation affecting the external parts of those two continents would account for the onset of their mutual tectonic interplays in their collisional course. The vergence of  $D_1$

structures in the study area is compatible with an upper plate position for the external margin of Gondwana at the beginning of the continental collision [Díez Fernández *et al.*, 2016].

From a regional tectonic point of view, D<sub>2</sub> thrusting can be interpreted as a stage of colder deformation associated with the amplification of overturned folds and subsequent exhumation to upper crustal depths. Shearing during latest D<sub>1</sub> would eventually fracture rocks and induce fault propagation under colder conditions, giving way to D<sub>2</sub> thrusts. The left-lateral component observed in these thrusts favors a transpressional model for their development [Expósito Ramos, 2005; Pérez-Cáceres *et al.*, 2016]. Moreover, the stretching lineation associated with D<sub>1</sub> folds is roughly parallel to their axes. Therefore, lateral tectonic flow is not just restricted to D<sub>2</sub>, but extends back to the onset of Variscan deformation. Such flow pattern has been interpreted as the consequence of an oblique collision between Gondwana and Laurussia [Martínez Catalán, 1990; Shelley and Bossière, 2000; Silva and Pereira, 2004; Díez Fernández and Martínez Catalán, 2012; Pérez-Cáceres *et al.*, 2016].

D<sub>3</sub> upright folds indicate a new shortening event for the study area. Equivalent folds exist throughout the internal zones of the Iberian Massif, and a tectonic origin (i.e. further convergence between Gondwana and Laurussia) has been proposed for these folds [e.g., Martínez Catalán, 2011]. D<sub>3</sub> folds have been dated at Moscovian-Gzhelian [~315-300 Ma; Ries, 1979; Martínez Poyatos, 2002; Expósito Ramos, 2005; Valle Aguado *et al.*, 2005; Díez Fernández and Pereira, 2017], and are frequently related to strike-slip shear zones formed in a transpressional setting [e.g., Iglesias Ponce de Leon and Choukroune, 1980].

In the study area, shortening during the three first Variscan phases gave way to extension (D<sub>4</sub>). SW Iberia is characterized by several phases of extension. An extensional stage featured by low-angle faulting and the onset of migmatite domes has been constrained to an age range of ~345–315 Ma [Díaz Azpiroz *et al.*, 2004; Pereira *et al.*, 2009, 2012a]. This deformation attenuates previous overthickened crust and predates the development of D<sub>3</sub>

strike-slip shear zones, which are followed by further extensional activity ( $D_4$ ) acting over a re-thickened orogenic crust.

#### *4.2 Obduction of the Calzadilla Ophiolite: tectonic model and regional implications*

In present-day coordinates, top-to-the-E tectonic transport represents a vector oblique to the main Variscan structures and boundaries between classical geotectonic zones of the Iberian Massif, which are widely accepted as representatives of different sections across the Gondwanan paleogeography. Since the boundaries between major geotectonic units in SW Iberia trend NW-SE (Fig. 2), E-directed Ediacaran thrusting in the study area would imply the transference of tectonic units towards inner sections of Gondwana, which would be represented by the Central Iberian Zone in a broad sense. Should the current regional trend of these boundaries be also oblique to the vector of ophiolite emplacement in Ediacaran times, thrust tectonics would have probably taken place during oblique sinistral convergence.

Ediacaran thrusting would have produced several juxtapositions of upper mantle rocks on top of sedimentary rocks. In this regard, higher strain is expected near zones adjacent to thrust surfaces. Remarkably, Ediacaran deformation in the Serie Negra Group is heterogeneous, the highest strained domains (including mylonites) being observed around the El Villar thrust imbricates. However, Ediacaran thrusting hardly explains why sedimentary rocks of the Serie Negra Group occur right on top of upper mantle rocks. This geometry can be explained if we admit the existence of either an unconformity and/or an extensional fault. Either of these two options would require another phase of deformation before the Ediacaran thrusting observed.

The main observations and inferences regarding the latest Ediacaran to the Early Cambrian tectonic evolution of the study area can be integrated in a model of an active margin that switches between extension-dominated and compression-dominated stages in the

upper plate (Fig. 9). Relative positioning of the sections across the Cadomian arc system are based on the widely accepted Ediacaran subduction polarity under Gondwana, and on the gradually more external position that the Ediacaran series of the Central Iberian Zone, then the Basal Allochthonous Units, and finally the Upper Allochthonous Units, occupied across the margin of Gondwana after restoring Variscan thrusting in the Iberian Massif [*Simancas et al.*, 2009; *Díez Fernández et al.*, 2016].

During most of the Ediacaran (c. 600-560 Ma), the southwestern part of the Upper Allochthon of the Ossa Morena Complex was located in the fore-arc region of an active continental arc (Fig. 9a). Infant subduction and extension in this section would have facilitated the generation of boninitic magmas (e.g., metagabbros from the Calzadilla Ophiolite; *Arenas et al.*, 2018) as well as the progressive widening of a fore-arc basin (deposition of Serie Negra fore-arc siliciclastic sediments; *Sánchez Lorda et al.*, 2014, 2016). Ongoing subduction would trigger serpentinization over the underlying mantle wedge in the fore-arc region. Significant extension in this context would explain the juxtaposition (via extensional detachments) of upper mantle and overlying sedimentary rocks in the fore-arc basin (Fig. 9b). The intra-arc sedimentary basins at this stage are probably represented by central to northeastern sections of the Upper Allochthon of the Ossa Morena Complex (e.g., Obejo-Valsequillo Domain), which feature voluminous, felsic, arc-related Ediacaran magmatism [e.g., *Bandrés et al.*, 2004; *Henriques et al.*, 2015]. A wide back-arc region for this system is represented by the Ediacaran series of the Basal Allochthonous Units of the Iberian Massif [*Díez Fernández et al.*, 2010, 2017; *Fuenlabrada et al.*, 2012], the Ediacaran series of the Central Iberian Zone [*Rodríguez-Alonso et al.*, 2004; *Villaseca et al.*, 2014; *Fuenlabrada et al.*, 2016], and of the West Asturian-Leonese Zone [*Fernández-Suárez et al.*, 1998; *Rubio-Ordóñez et al.*, 2015].

In the latest Ediacaran, the whole fore-arc region of the Cadomian arc system was subjected to subhorizontal contraction, which was resolved via thrusting in the case of the study area. Thrusting in this setting was directed inland onto Gondwana, and drove the obduction of (serpentinized) upper mantle-lower crust sections of the fore-arc (Calzadilla Ophiolite; Fig. 9c). Such obduction direction suggests positive buoyancy of the fore-arc section and therefore reluctance to be incorporated into an accretionary prism located nearby. The younger age of the fore-arc crust relative to the age of the subducting (denser?) oceanic crust that could be arriving to the trench, and a significant serpentinization (and therefore a drop in rock density) of the fore-arc upper mantle induced by ongoing subduction are two essential parameters to consider. Accordingly, the fore-arc would represent a more buoyant section in the arc-trench system, and so it may have escaped accretion and be pushed away from the trench upon superimposed compression. This evolution resembles models proposed for the Nevadan Orogeny in the North American Pacific coast and the obduction of the Great Valley Ophiolite [Godfrey *et al.*, 1997; Wakabayashi and Dilek, 2003], or the obduction of the Duarte – Loma Caribe fore-arc ophiolite in the Greater Antillean arc [Draper *et al.*, 1996].

Ediacaran subhorizontal contraction in the intra-arc and back-arc sections has been also documented in the Iberian Massif. Although no major thrusts have been described in those parts of the arc system, there exists evidence for the development of regional unconformities between Early Cambrian to Ordovician strata and underlying and folded Ediacaran basement rocks [e.g., Llopis *et al.*, 1970; Capdevila *et al.*, 1971; Díez Balda, 1986; Pieren Pidal, 2000; Martínez Poyatos *et al.*, 2001]. Some of those unconformities developed during the Precambrian, most likely during the latest Ediacaran [e.g., Talavera *et al.*, 2015].

Coupling and decoupling between upper and lower plate in subduction zones may explain the switching between compression-dominated and extension-dominated stages in

arc-systems [Uyeda and Kanamori, 1979; Jarrard, 1986]. In the overriding plate, periods dominated by compressional stresses (e.g., obduction of the Calzadilla Ophiolite, folding and thrusting? in the back-arc) would correspond to stages of tight coupling [e.g., Jordan, 1995; Allmendinger et al., 1997] (Fig. 9b), whereas plate decoupling brings about periods dominated by extension into the arc-trench system [Taylor and Karner, 1983; Stern and Bloomer, 1992]. In this regard, the development of a wide back-arc region and the (hyper-) extension of the fore-arc that took place before latest Ediacaran compression, can be ascribed to a decoupling stage in the arc system (Fig. 9a). This stage would have favored the deposition of thick successions of siliciclastic rocks within subsiding arc-related basins along the periphery of Gondwana (e.g., Serie Negra Group of SW Iberia, Schist-Greywacke Complex of the Central Iberian Zone, etc.), all of which were subsequently deformed once intervening tectonic plates switched to a coupling stage. An increase in convergence rate, a significant decrease in the dip of the subducting plate (i.e. flat-subduction), or the arrival of younger, more buoyant lithosphere to the trench are possible causes that explain the change to a coupled state between plates [Stern, 2002 and references therein]. Geotectonic models for the northern margin of Gondwana during the latest Ediacaran – Early Cambrian foresee a progressive flattening of the subducting plate due to the proximity of a mid-ocean ridge, or the arrival of seamounts or oceanic plateaus, to the subduction zone [e.g., Sánchez-García et al., 2003; Nance et al., 2010; Stampfli et al., 2013].

Continental arc andesites, such as those from the Malcocinado Formation [Sánchez-Carretero et al., 1989; Pin et al., 2002], covering Precambrian rock sequences previously located at external sections of the arc-trench system (fore-arc), suggest either steeper subduction relative to previous stages and/or the migration of the trench outwards from the continental arc (slab retreat). Both scenarios require ongoing subduction, and would imply

rapid subsidence and extension in the upper plate. The two first are conditions necessary to explain the main features of the Malcocinado Formation sedimentary and magmatic record.

The development of an arc-related basin and supra-subduction zone magmatism after the emplacement of the Calzadilla Ophiolite (Malcocinado Formation) suggest that subduction either resumed or did not cease but changed its parameters during the Ediacaran-Cambrian transition. The first option would imply that subduction ceased during the latest Ediacaran, and the compression-dominated stage in the overriding plate should be related to a process other than subduction. The second and preferred option considers a flat(er)-subduction during the latest Ediacaran that evolves to a setting where the dip of the subduction plane increases progressively, thus facilitating partial decoupling between upper and lower plates (Fig. 9c). The younger (maximum depositional) age considered for the Malcocinado Formation ( $522 \pm 8$  Ma; *Ordóñez-Casado et al.*, 1998) matches, within error, with the c. 530-525 Ma age for the onset of migmatite domes [*Eguíluz and Abalos*, 1992; *Expósito et al.*, 2003; *Simancas et al.*, 2004] and extension-related magmatism in SW Iberia [*Schäfer*, 1990; *Ochsner*, 1993; *Ordóñez Casado*, 1998; *Ordóñez-Casado et al.*, 1998; *Romeo et al.*, 2006; *Chichorro et al.*, 2008; *Sánchez-García et al.*, 2008]. It also approaches the age of the onset of Cambrian tilting of the study area. Magmatism following the continental arc andesites has been interpreted as transitional to a rifting stage [*Sánchez-García et al.*, 2014]. However, this magmatism has tonalitic and leucogranitic end-members, lacks mafic or mantle-derived components, shows Eu and significant Nb negative anomalies, plots into the Volcanic Arc Granites field of *Pearce et al.* [1984b], and shows trends typical of calc-alkaline series [Early Rift-Related Event; *Sánchez-García et al.*, 2008], i.e. it is largely compatible with active subduction. Overall, an extension-dominated stage developed after the emplacement of the Calzadilla Ophiolite. We favor that this stage in the arc-system was coeval with subduction, and that extension in the overriding plate was probably associated

with its progressive decoupling from the lower plate (i.e. subduction did not cease during the Cambrian). Either a steeper subduction and/or slab retreat during the latest Ediacaran – Early Cambrian would result in an incursion of a mantle wedge under the previously thickened crust (Fig. 9c), thus triggering partial melting and the onset of migmatite domes [*Expósito et al.*, 2003; *Sánchez-García et al.*, 2003].

Besides explaining the synchrony between an extension-dominated stage and subduction-related magmatism, the slab roll-back (slab retreat) model allows a reconciliation of other data across the Iberian Massif. The Central Iberian and West Asturian-Leonese zones, located in a closer position relative to mainland Gondwana, represent a broad back-arc region of the Cadomian arc-system in Ediacaran times. However, the location of the back-arc of this system moved from that position to a more external one in Cambrian times, as evidenced by the development of a new back-arc spreading center (featured by the generation of oceanic transitional crust) in a more external position, such as that represented by the Cambrian, back-arc ophiolites and related sedimentary record preserved in the Variscan Allochthonous Complexes [*Arenas et al.*, 2007; *Díez Fernández et al.*, 2010]. The migration of the back-arc region to a more external position across the continental margin is compatible with either an oceanward migration of the trench and/or a steepening of the subducting plate, both of which are expected in a slab retreat process.

## 5. Conclusions

Qualitative and simplified unstraining of Variscan (Devonian-Carboniferous) deformation in a section of SW Iberia has allowed the identification and analysis of Ediacaran and Cambrian deformation that affected the outer sections of Gondwana during the waning stages of the Cadomian Orogeny. The main phase of Cadomian deformation is latest Ediacaran, and is related to the obduction of a fore-arc ophiolite towards inland Gondwana

(Calzadilla Ophiolite). This event represents a turning point in the geodynamic evolution of the African margin of Gondwana, as it separates two extension-dominated periods recorded in the upper plate of the Cadomian orogen, each leading to rather contrasting settings. The pre-obduction extensional period facilitated the onset and widening of fore-arc and back-arc basins in the external part of the continent, while the post-obduction period brought about the onset of extensional migmatitic domes, an outboard migration of back-arc spreading centers across peri-Gondwana, and the eventual opening of a major basin such as the Rheic Ocean. We suggest that the ongoing subduction beneath Gondwana seems to have played a key role in the whole process. Changes in the parameters of subduction (convergence rate, dip and buoyancy of the subducting plate) during the Ediacaran – Cambrian transition may explain the switches between extension-dominated and compression-dominated stages in the upper plate, as they could ultimately induce coupling and decoupling between subducting and upper plate in the Cadomian arc-trench system. Periods of extension in the arc-trench system are compatible with decoupling and slab retreat, whereas periods of compression suggest strong slab coupling and flatter subduction.

## **6. Acknowledgments**

We would like to thank Rob Strachan and four anonymous referees for valuable reviews. Financial support has been provided by the Spanish project CGL2016-76438-P (Ministerio de Economía, Industria y Competitividad). This work is a contribution to IGCP project 648 (Supercontinent Cycle and Global Geodynamics). The data used are listed in the references, figures, and supplements.

## 7. References

Abalos, B., J. I. Gil Ibarguchi, and L. Eguiluz (1991), Cadomian subduction, collision and Variscan transpression in the Badajoz-Cordoba Shear Belt, Southwest Spain, *Tectonophysics*, 199, 51-72.

Abati, J., A. Gerdes, J. Fernández-Suárez, R. Arenas, M. J. Whitehouse, and R. Díez Fernández (2010), Magmatism and early-Variscan continental subduction in the northern Gondwana margin recorded in zircons from the basal units of Galicia, NW Spain, *Geological Society of America Bulletin*, 122, 219-235.

Aguayo Fernández, J. M. (1985), Rocas ultramáficas en el sector de Calzadilla de los Barros (Badajoz), MSc thesis, 110 pp, Universidad del País Vasco, Bilbao.

Albert, R., R. Arenas, A. Gerdes, S. Sánchez Martínez, and L. Marko (2015a), Provenance of the high-P and high-T unit of the Cabo Ortegal Complex (NW Iberian Massif), *Journal of Metamorphic Geology*, 33, 959-979.

Albert, R., R. Arenas, A. Gerdes, S. Sánchez Martínez, J. Fernández-Suárez, and J. M. Fuenlabrada (2015b), Provenance of the Variscan Upper Allochthon (Cabo Ortegal Complex, NW Iberian Massif), *Gondwana Research*, 28, 1434-1448.

Alia, M. (1963), Rasgos estructurales de la Baja Extremadura, *Boletín Real Sociedad Española Historia Natural*, 61, 247-262.

Allmendinger, R. W., T. E. Jordan, S. M. Kay, and B. L. Isacks (1997), The evolution of the Altiplano-Puna Plateau of the central Andes, *Annual Review of Earth and Planetary Sciences*, 25, 139-174.

Andonaegui, P., J. Abati, and R. Díez Fernández (2017), Late Cambrian magmatic arc activity in peri-Gondwana: geochemical evidence from the Basal Allochthonous Units of NW Iberia, *Geologica Acta*, 15(4), 305-321.

- Arenas, R., J. R. Martínez Catalán, S. Sánchez Martínez, J. Fernández-Suárez, P. Andonaegui, J. A. Pearce, and F. Corfú (2007), The Vila de Cruces ophiolite: A remnant of the early Rheic Ocean in the Variscan suture of Galicia (northwest Iberian Massif), *The Journal of Geology*, 115, 129-148.
- Arenas, R., et al. (2018), The Calzadilla Ophiolite (SW Iberia) and the Ediacaran fore-arc evolution of the African margin of Gondwana, *Gondwana Research*, 58, 71-86.
- Arriola, A., L. A. Cueto, J. Fernández-Carrasco, and A. Garrote (1984), Serpentinitas y mineralizaciones de cromo asociadas en el Proterozoico superior de Ossa-Morena, *Cuadernos do Laboratorio Xeolóxico de Laxe*, 8, 137-145.
- Azor, A., F. Gonzalez Lodeiro, and J. F. Simancas (1993), Cadomian subduction/collision and Variscan transpression in the Badajoz-Córdoba Shear Belt, southwest Spain: a discussion on the age of the main tectonometamorphic events, *Tectonophysics*, 217, 343-346.
- Ballèvre, M., E. Le Goff, and R. Hébert (2001), The tectonothermal evolution of the Cadomian belt of northern Brittany, France: a Neoproterozoic volcanic arc, *Tectonophysics*, 331(1), 19-43.
- Bandrés, A., L. Eguíluz, C. Pin, J. L. Paquette, B. Ordóñez, B. Le Fèvre, L. A. Ortega, and J. I. Gil Ibarguchi (2004), The northern Ossa-Morena Cadomian batholith (Iberian Massif): magmatic arc origin and early evolution, *International Journal of Earth Sciences*, 93, 860-885.
- Blatrix, P., and J. P. Burg (1981),  $^{40}\text{Ar}/^{39}\text{Ar}$  dates from Sierra Morena (southern Spain): Variscan metamorphism and Cadomian Orogeny, *Neues Jahrbuch Mineral Monatshefte*, 10, 470-478.
- Braid, J. A., J. B. Murphy, C. Quesada, and J. Mortensen (2011), Tectonic escape of a crustal fragment during the closure of the Rheic Ocean: U-Pb detrital zircon data from the

Late Palaeozoic Pulo do Lobo and South Portuguese zones, southern Iberia, *Journal of the Geological Society*, 168, 383-392.

Brandon, M. T., M. K. Roden-Tice, and J. I. Garver (1998), Late Cenozoic exhumation of the Cascadia accretionary wedge in the Olympic Mountains, northwest Washington state, *Geological Society of America Bulletin*, 110, 985-1009.

Brown, M., G. M. Power, C. G. Topley, and R. S. D'Lemos (1990), Cadomian magmatism in the North Armorican Massif, *Geological Society, London, Special Publications*, 51(1), 181-213.

Capdevila, R., P. Matte, and J. Paredes (1971), La nature du Précambrien et ses relations avec le Paléozoïque dans la Sierra Morena centrale (Sud de l'Espagne), *Comptes Rendus de l'Académie des Sciences de Paris*, 273, 1359-1362.

Carvalhosa, A. (1965), Contribuição para o conhecimento geológico da região entre Portel e Ficalho (Alentejo), *Memórias dos Serviços Geológicos de Portugal*, 11, 1-130.

Castro, A., A. García-Casco, C. Fernández, L. G. Corretgé, I. Moreno-Ventas, T. Gerya, and I. Löw (2009), Ordovician ferrosilicic magmas: Experimental evidence for ultrahigh temperatures affecting a metagreywacke source, *Gondwana Research*, 16(3), 622-632.

Condie, K. C., and V. Pease (2008), When did Plate Tectonics Begin on Planet Earth?, *Geological Society of America, Special Paper*, 440, 1-294.

Crowley, Q. G., P. A. Floyd, J. A. Winchester, W. Franke, and J. G. Holland (2000), Early Palaeozoic rift-related magmatism in Variscan Europe: fragmentation of the Armorican Terrane Assemblage, *Terra Nova*, 12, 171-180.

Chantraine, J., E. Egal, D. Thiéblemont, E. Le Goff, C. Guerrot, M. Ballèvre, and P. Guennoc (2001), The Cadomian active margin (North Armorican Massif, France): a segment of the North Atlantic Panafrikan belt, *Tectonophysics*, 331, 1-18.

Chichorro, M., M. F. Pereira, M. Díaz-Azpiroz, I. S. Williams, C. Fernández, C. Pin, and J. B. Silva (2008), Cambrian ensialic rift-related magmatism in the Ossa-Morena Zone (Évora-Aracena metamorphic belt, SW Iberian Massif): Sm–Nd isotopes and SHRIMP zircon U–Th–Pb geochronology, *Tectonophysics*, *461*, 91-113.

Dallmeyer, R. D., and C. Quesada (1992), Cadomian vs. Variscan evolution of the Ossa-Morena zone (SW Iberia): field and  $^{40}\text{Ar}/^{39}\text{Ar}$  mineral age constraints, *Tectonophysics*, *216*, 339-364.

D’Lemos, R. S., R. A. Strachan, and C. G. Topley (1990), *The Cadomian Orogeny*.

Dewey, J. F. (1976), Ophiolite obduction, *Tectonophysics*, *31*, 93-120.

Díaz Azpiroz, M., C. Fernández, A. Castro, and M. El-Biad (2006), Tectonometamorphic evolution of the Aracena metamorphic belt (SW Spain) resulting from ridge-trench interaction during Variscan plate convergence, *Tectonics*, *25*, TC1001.

Díaz Azpiroz, M., A. Castro, C. Fernández, S. López, J. C. Fernández Caliani, and I. Moreno-Ventas (2004), The contact between the Ossa Morena and the South Portuguese zones. Characteristics and significance of the Aracena metamorphic belt, in its central sector between Aroche and Aracena (Huelva), *Journal of Iberian Geology*, *30*, 23-51.

Díez Balda, M. A. (1986), El Complejo Esquisto-Grauváquico, las series paleozoicas y la estructura hercínica al Sur de Salamanca, 162 pp, Universidad de Salamanca, Salamanca.

Díez Fernández, R., and J. R. Martínez Catalán (2012), Stretching lineations in high-pressure belts: the fingerprint of subduction and subsequent events (Malpica–Tui complex, NW Iberia), *Journal of the Geological Society*, *169*, 531-543.

Díez Fernández, R., and R. Arenas (2015), The Late Devonian Variscan suture of the Iberian Massif: A correlation of high-pressure belts in NW and SW Iberia, *Tectonophysics*, *654*, 96-100.

Díez Fernández, R., and M. F. Pereira (2016), Extensional orogenic collapse captured by strike-slip tectonics: constraints from structural geology and U-Pb geochronology of the Pinhel shear zone (Variscan orogen, Iberian Massif), *Tectonophysics*, 691(Part B), 290-310.

Díez Fernández, R., and M. F. Pereira (2017), Strike-slip shear zones of the Iberian Massif: are they coeval?, *Lithosphere*, 9(5), 726-744.

Díez Fernández, R., P. Castiñeiras, and J. Gómez Barreiro (2012), Age constraints on Lower Paleozoic convection system: magmatic events in the NW Iberian Gondwana margin, *Gondwana Research*, 21, 1066-1079.

Díez Fernández, R., M. F. Pereira, and D. A. Foster (2015), Peralkaline and alkaline magmatism of the Ossa-Morena zone (SW Iberia): Age, source, and implications for the Paleozoic evolution of Gondwanan lithosphere, *Lithosphere*, 7, 73-90.

Díez Fernández, R., J. R. Martínez Catalán, A. Gerdes, J. Abati, R. Arenas, and J. Fernández-Suárez (2010), U-Pb ages of detrital zircons from the Basal allochthonous units of NW Iberia: Provenance and paleoposition on the northern margin of Gondwana during the Neoproterozoic and Paleozoic, *Gondwana Research*, 18, 385-399.

Díez Fernández, R., J. M. Fuenlabrada, M. Chichorro, M. F. Pereira, S. Sánchez Martínez, J. B. Silva, and R. Arenas (2017), Geochemistry and tectonostratigraphy of the basal allochthonous units of SW Iberia (Évora Massif, Portugal): keys to the reconstruction of pre-Pangean paleogeography in southern Europe, *Lithos*, 268-271, 285-301.

Díez Fernández, R., R. Arenas, M. F. Pereira, S. Sánchez Martínez, R. Albert, L. M. Martín Parra, F. J. Rubio Pascual, and J. Matas (2016), Tectonic evolution of Variscan Iberia: Gondwana - Laurussia collision revisited, *Earth-Science Reviews*, 162, 269-292.

Draper, G., G. Gutiérrez, and J. F. Lewis (1996), Thrust emplacement of the Hispaniola peridotite belt: Orogenic expression of the mid-Cretaceous Caribbean arc polarity reversal?, *Geology*, 24(12), 1143-1146.

Edwards, S. J., W. P. Schellart, and J. C. Duarte (2015), Geodynamic models of continental subduction and obduction of overriding plate forearc oceanic lithosphere on top of continental crust, *Tectonics*, 34, 1494-1515.

Eguiluz, L., A. Apraiz, L. M. Martínez-Torres, and T. Palacios (1997), Estructura del sector de Zafra: implicaciones en la subdivisión de unidades Cámbricas de la Zona de Ossa Morena (ZOM), *Geogaceta*, 22, 59-62.

Eguiluz, L. (1987), Petrogénesis de rocas ígneas y metamórficas en el Antiforme Burguillos-Monesterio, Macizo Ibérico Meridional, Ph.D. thesis, 694 pp, Universidad del País Vasco.

Eguiluz, L., and B. Abalos (1992), Tectonic setting of Cadomian low-pressure metamorphism in the central Ossa-Morena zone (Iberian massif, SW Spain), *Precambrian Research*, 56, 113-137.

Eguiluz, L., J. I. Gil Ibarguchi, B. Abalos, and A. Apraiz (2000), Superposed Hercynian and Cadomian orogenic cycles in the Ossa-Morena zone and related areas of the Iberian Massif, *Geological Society of America Bulletin*, 112, 1398-1413.

El Hadi, H., J. F. Simancas, D. Martínez-Poyatos, A. Azor, A. Tahiri, P. Montero, C. M. Fanning, F. Bea, and F. González-Lodeiro (2010), Structural and geochronological constraints on the evolution of the Bou Azzer Neoproterozoic ophiolite (Anti-Atlas, Morocco), *Precambrian Research*, 182(1), 1-14.

Expósito, I., J. F. Simancas, F. González Lodeiro, F. Bea, P. Montero, and K. Salman (2003), Metamorphic and deformational imprint of Cambrian-Lower Ordovician rifting in the Ossa-Morena Zone (Iberian Massif, Spain), *Journal of Structural Geology*, 25, 2077-2087.

Expósito Ramos, I. (2005), Evolución estructural de la mitad septentrional de la Zona de Ossa-Morena y su relación con el límite Zona Ossa-Morena/Zona Centroibérica, *Nova Terra*, 27, 1-286.

- Fernández-Carrasco, J., J. M. Portero García, A. Garrote, A. Arriola, L. Eguíluz, R. Sánchez-Carretero, C. Quesada, and L. A. Cueto (1980), Mapa y memoria de la Hoja nº 876 (Fuente de Cantos) del Mapa Geológico de España, Escala 1/50.000, *Instituto Geológico y Minero de España*.
- Fernández-Suárez, J., G. Gutiérrez-Alonso, and T. E. Jeffries (2002), The importance of along-margin terrane transport in northern Gondwana: insights from detrital zircon parentage in Neoproterozoic rocks from Iberia and Brittany, *Earth and Planetary Science Letters*, 204, 75-88.
- Fernández-Suárez, J., G. Gutiérrez-Alonso, G. A. Jenner, and S. E. Jackson (1998), Geochronology and geochemistry of the Pola de Allande granitoids (northern Spain): their bearing on the Cadomian-Avalonian evolution of northwest Iberia, *Canadian Journal of Earth Sciences*, 35, 1439-1453.
- Fricke, W. (1941), Die Geologie des Grenzgebietes zwischen nordstlicher Sierra Morena und Extremadura, PhD thesis, 91 pp, Berlin University, Berlin.
- Fuenlabrada, J. M., A. P. Pieren, R. Díez Fernández, S. Sánchez Martínez, and R. Arenas (2016), Geochemistry of the Ediacaran-Early Cambrian transition in Central Iberia: Tectonic setting and isotopic sources, *Tectonophysics*, 681, 15-30.
- Fuenlabrada, J. M., R. Arenas, R. Díez Fernández, S. Sánchez Martínez, J. Abati, and A. López Carmona (2012), Sm–Nd isotope geochemistry and tectonic setting of the metasedimentary rocks from the basal allochthonous units of NW Iberia (Variscan suture, Galicia), *Lithos*, 148, 196-208.
- Galindo, C., C. Casquet, M. R. Portugal Ferreira, and C. A. Regencio Macedo (1986), O Complexo Plutónico de Táliga-Barcarrota - Um Complexo intrusivo com Idades Caledónica e Hercínica, *Maleo. Boletim Informativo da Sociedade Geológica de Portugal. II Congresso Nacional de Geologia de Portugal, Lisboa, Volume 2, number 13, 22.*

Galindo, C., C. Casquet, M. R. Portugal Ferreira, and C. A. Regencio Macedo (1987), Geocronología del Complejo plutónico Táliga-Barcarrota (CPTB). Badajoz, España, in: Geología de los granitoides y rocas asociadas del Macizo Hespérico. Libro Homenaje a L.C. García de Figuerola, edited by F. Bea, A. Carnicero, J. C. Gonzalo, M. López-Plaza and M. D. Rodríguez Alonso, pp. 385-392, Ed. Rueda.

García-Arias, M., A. Díez-Montes, C. Villaseca, and I. F. Blanco-Quintero (2018), The Cambro-Ordovician Ollo de Sapo magmatism in the Iberian Massif and its Variscan evolution: A review, *Earth-Science Reviews*, 176, 345-372.

Godfrey, N. J., B. C. Beaudoin, and S. L. Klemperer (1997), Ophiolitic basement to the Great Valley forearc basin, California, from seismic and gravity data: Implications for crustal growth at the North American continental margin, *Geological Society of America Bulletin*, 109(12), 1536-1562.

Gonçalves, F. (1971), Subsídios para o Conhecimento Geológico do Nordeste Alentejano, *Servicios Geológicos de Portugal, Memória (Nova Série)*, 18, 1-62.

Henriques, S. B. A., A. M. R. Neiva, M. L. Ribeiro, G. R. Dunning, and L. Tajčmanová (2015), Evolution of a Neoproterozoic suture in the Iberian Massif, Central Portugal: New U-Pb ages of igneous and metamorphic events at the contact between the Ossa Morena Zone and Central Iberian Zone, *Lithos*, 220–223, 43-59.

Iglesias Ponce de Leon, M., and P. Choukroune (1980), Shear zones in the Iberian arc, *Journal of Structural Geology*, 2, 63-68.

Jarrard, R. D. (1986), Relations among subduction parameters, *Reviews of Geophysics*, 24(2), 217-284.

Jiménez-Díaz, A. (2008), Análisis de los procesos de cizalla dúctil en el macizo peridotítico de Calzadilla de los Barros (Extremadura), MSc thesis, 51 pp, Universidad Complutense, Madrid, Spain.

- Jiménez-Díaz, A., R. Capote, R. Tejero, R. Lunar, L. Ortega, S. Monterrubio, C. Maldonado, and D. Rodríguez (2009), La fábrica de las rocas miloníticas de la zona de cizalla de Los Llanos (Calzadilla de los Barros, Badajoz), *Geogaceta*, 46, 27-30.
- Jordan, T. E. (1995), Retroarc Foreland and Related Basins, in *Tectonics of Sedimentary Basins*, edited by C. Busby and R. Ingersoll, pp. 331-362, Blackwell Scientific Publications.
- Kounov, A., J. Graf, A. von Quadt, D. Bernoulli, J.-P. Burg, D. Seward, Z. Ivanov, and M. Fanning (2012), Evidence for a “Cadomian” ophiolite and magmatic-arc complex in SW Bulgaria, *Precambrian Research*, 212-213, 275-295.
- Linnemann, U., A. Gerdes, K. Drost, and B. Buschmann (2007), The continuum between Cadomian orogenesis and opening of the Rheic Ocean: Constraints from LA-ICP-MS U–Pb zircon dating and analysis of plate-tectonic setting (Saxo-Thuringian zone, northeastern Bohemian Massif, Germany), in *The evolution of the Rheic Ocean: From Avalonian-Cadomian active margin to Alleghenian-Variscan collision*, edited by U. Linnemann, R. D. Nance, P. Kraft and G. Zulauf, pp. 61-96, doi: 10.1130/2007.2423(1103), Geological Society of America Special Paper.
- Linnemann, U., F. Pereira, T. E. Jeffries, K. Drost, and A. Gerdes (2008), The Cadomian Orogeny and the opening of the Rheic Ocean: The diachrony of geotectonic processes constrained by LA-ICP-MS U–Pb zircon dating (Ossa-Morena and Saxo-Thuringian Zones, Iberian and Bohemian Massifs), *Tectonophysics*, 461, 21-43.
- Liñán, E. (1978), Bioestratigrafía de la Sierra de Córdoba, PhD thesis, 212 pp, Universidad de Granada, Granada.
- Liñán, E. (1984), Los icnofósiles de la Formación Torreárboles (¿Precámbrico?-Cámbrico Inferior) en los alrededores de Fuente de Cantos, Badajoz, *Cuadernos do Laboratorio Xeolóxico de Laxe*, 8, 47-74.

Liñán, E., and T. Palacios (1983), Aportaciones micropaleontológicas para el conocimiento del límite Precámbrico-Cámbrico en la Sierra de Córdoba, España, *Comunicações dos Serviços Geológicos de Portugal*, 69, 227-234.

Liñán, E., and C. Quesada (1990), Ossa-Morena Zone: 2. Stratigraphy. Rift phase, in *Pre-Mesozoic Geology of Iberia*, edited by R. D. Dallmeyer and E. Martínez García, pp. 259–266, Springer-Verlag, Berlin, Germany.

Liñán, E., T. Palacios, and A. Perejón (1984), Precambrian—Cambrian boundary and correlation from southwestern and central part of Spain, *Geological Magazine*, 121(3), 221-228.

Liñán, E., A. Perejón, and K. Sdzuy (1993), The Lower—Middle Cambrian stages and stratotypes from the Iberian Peninsula: a revision, *Geological Magazine*, 130(6), 817-833.

Llopis, N., M. A. San José, and P. Herranz (1970), Notas sobre una discordancia posiblemente precámbrica al SE de la provincia de Badajoz y sobre la edad de las series paleozoicas circundantes, *Boletín Geológico Minero*, 81, 586-592.

Martínez Catalán, J. R. (1990), A non-cylindrical model for the northwest Iberian allochthonous terranes and their equivalents in the Hercynian belt of Western Europe, *Tectonophysics*, 179, 253-272.

Martínez Catalán, J. R. (2011), Are the oroclines of the Variscan belt related to late Variscan strike-slip tectonics?, *Terra Nova*, 23, 241-247.

Martínez Poyatos, D., F. González Lodeiro, A. Azor, and J. F. Simancas (2001), La estructura de la Zona Centroibérica en la región de Los Pedroches (Macizo Ibérico meridional), *Revista de la Sociedad Geológica de España*, 14, 147-160.

Martínez Poyatos, D. J. (2002), Estructura del borde meridional de la Zona Centroibérica y su relación con el contacto entre las Zonas Centroibérica y de Ossa-Morena, *Nova Terra*, 18, 1-295.

Martos, R., L. Ortega, F. Gervilla, R. Piña, S. Monterrubio, R. Lunar, and H. Albert (2010), Caracterización químico-mineralógica de las cromititas ofiolíticas de Calzadilla de los Barros (Badajoz), *Geogaceta*, 48, 175-178.

Matte, P. (1991), Accretionary history and crustal evolution of the Variscan belt in Western Europe, *Tectonophysics*, 196, 309-337.

Merinero, R., R. Lunar, L. O. Menor, R. P. García, S. Monterrubio, and F. Gervilla (2013), Hydrothermal palladium enrichment in podiform chromitites of Calzadilla de los Barros (SW Iberian Peninsula), *The Canadian Mineralogist*, 51, 387-404.

Merinero, R., R. Lunar, L. Ortega, R. Piña, S. Monterrubio, and F. Gervilla (2014), Zoned chromite records multiple metamorphic episodes in the Calzadilla de los Barros ultramafic bodies (SW Iberian Peninsula), *European Journal of Mineralogy*, 26(6), 757-770.

Montero, P., F. Bea, F. González Lodeiro, C. Talavera, and M. J. Whitehouse (2007), Zircon ages of the metavolcanic rocks and metagranites of the Ollo de Sapo Domain in central Spain: implications for the neoproterozoic to early palaeozoic evolution of Iberia, *Geological Magazine*, 144, 963-976.

Monterrubio, S. (1991), Mineralizaciones asociadas a rocas ultrabásicas en el Hercínico español, PhD thesis, 323 pp, Universidad Complutense, Madrid.

Murphy, J. B., G. Gutiérrez-Alonso, R. D. Nance, J. Fernández-Suárez, J. D. Keppie, C. Quesada, R. A. Strachan, and J. Dostal (2006), Origin of the Rheic Ocean: Rifting along a Neoproterozoic suture?, *Geology*, 34, 325-328.

Nance, R. D., G. Gutiérrez-Alonso, J. D. Keppie, U. Linnemann, J. B. Murphy, C. Quesada, R. A. Strachan, and N. H. Woodcock (2010), Evolution of the Rheic Ocean, *Gondwana Research*, 17, 194-222.

Ochsner, A. (1993), U – Pb Geochronology of the Upper Proterozoic – Lower Paleozoic geodynamic evolution in the Ossa-Morena Zone (SW Iberia): constraints on the timing of the Cadomian Orogeny, PhD thesis, 249 pp, ETH, Zurich, Switzerland.

Ordóñez-Casado, B., D. Gebauer, and L. Eguiluz (1998), SHRIMP age-constraints for the calc-alkaline volcanism in the Olivenza-Monesterio Antiform (Ossa-Morena, SW Spain), *Mineralogical magazine*, 62A, 1112-1113.

Ordóñez Casado, B., D. Gebauer, and L. Eguíluz (2009), Zircon Ion-Probe Dating the Maximum Age of Deposition of the Montemolín Succession (Lower Serie Negra) in the Ossa Morena Zone, Spain, *Macla*, 11, 137-138.

Ordóñez Casado, B. (1998), Geochronological studies of the Pre-Mesozoic basement of the Iberian Massif: the Ossa Morena zone and the Allochthonous Complexes within the Central Iberian zone, PhD thesis, 235 pp, Swiss Federal Institute of Technology, Zürich, Switzerland.

Palacios, T. (1989), Microfósiles de pared orgánica del Proterozoico Superior (región central de la Península Ibérica), *Memorias del Museo Paleontológico de la Universidad de Zaragoza*, 3(2), 1-91.

Passchier, C. W. (1997), The fabric attractor, *Journal of Structural Geology*, 19, 113-127.

Pearce, J. A., S. J. Lippard, and S. Roberts (1984a), Characteristics and tectonic significance of supra-subduction zone ophiolites, *Geological Society, London, Special Publications*, 16(1), 77-94.

Pearce, J. A., N. B. W. Harris, and A. G. Tindle (1984b), Trace Element Discrimination Diagrams for the Tectonic Interpretation of Granitic Rocks, *Journal of Petrology*, 25(4), 956-983.

- Pereira, M. F. (2015), Potential sources of Ediacaran strata of Iberia: a review, *Geodinamica Acta*, 27(1), 1-14.
- Pereira, M. F., M. Chichorro, U. Linnemann, L. Eguiluz, and J. B. Silva (2006), Inherited arc signature in Ediacaran and Early Cambrian basins of the Ossa-Morena Zone (Iberian Massif, Portugal): Paleogeographic link with European and North African Cadomian correlatives, *Precambrian Research*, 144, 297-315.
- Pereira, M. F., M. Chichorro, J. B. Silva, B. Ordóñez-Casado, J. K. W. Lee, and I. S. Williams (2012a), Early carboniferous wrenching, exhumation of high-grade metamorphic rocks and basin instability in SW Iberia: Constraints derived from structural geology and U–Pb and <sup>40</sup>Ar–<sup>39</sup>Ar geochronology, *Tectonophysics*, 558-559, 28-44.
- Pereira, M. F., A. R. Solá, M. Chichorro, L. Lopes, A. Gerdes, and J. B. Silva (2012b), North-Gondwana assembly, break-up and paleogeography: U–Pb isotope evidence from detrital and igneous zircons of Ediacaran and Cambrian rocks of SW Iberia, *Gondwana Research*, 22, 866 - 881.
- Pereira, M. F., M. Chichorro, I. S. Williams, J. B. Silva, C. Fernández, M. Díaz-Azpiroz, A. Apraiz, and A. Castro (2009), Variscan intra-orogenic extensional tectonics in the Ossa-Morena Zone (Évora-Aracena-Lora del Río metamorphic belt, SW Iberian Massif): SHRIMP zircon U–Th–Pb geochronology, *Geological Society, London, Special Publications*, 327, 215-237.
- Pérez-Cáceres, I., D. Martínez Poyatos, J. F. Simancas, and A. Azor (2017), Testing the Avalonian affinity of the South Portuguese Zone and the Neoproterozoic evolution of SW Iberia through detrital zircon populations, *Gondwana Research*, 42, 177-192.
- Pérez-Cáceres, I., J. F. Simancas, D. Martínez Poyatos, A. Azor, and F. González Lodeiro (2016), Oblique collision and deformation partitioning in the SW Iberian Variscides, *Solid Earth*, 7, 857-872.

Pieren Pidal, A. P. (2000), Las sucesiones anteordovícicas de la región oriental de la provincia de Badajoz y área contigua de la de Ciudad Real, 381 pp, Universidad Complutense de Madrid, Madrid, Spain.

Pin, C., E. Liñan, E. Pascual, T. Donaire, and A. Valenzuela (2002), Late Neoproterozoic crustal growth in the European Variscides: Nd isotope and geochemical evidence from the Sierra de Cordoba Andesites (Ossa-Morena Zone, Southern Spain), *Tectonophysics*, 352, 133-151.

Quesada, C. (1990), Precambrian successions in SW Iberia: their relationship to 'Cadomian' orogenic events, in *The Cadomian Orogeny*, edited by D. R. Lemos, R. A. Strachan and C. G. Topley, pp. 353-362, Geological Society, London, Special Publication.

Quesada, C. (1991), Geological constraints on the Paleozoic tectonic evolution of tectonostratigraphic terranes in the Iberian Massif, *Tectonophysics*, 185, 225-245.

Quesada, C. (2006), The Ossa-Morena Zone of the Iberian Massif: a tectonostratigraphic approach to its evolution, *Zeitschrift der Deutschen Gesellschaft für Geowissenschaften*, 157(4), 585-595.

Quesada, C., F. Bellido, R. D. Dallmeyer, I. Gil-Ibarguchi, J. T. Oliveira, A. Perez-Estaun, A. Ribeiro, M. Robardet, and J. B. Silva (1991), Terranes within the Iberian Massif: Correlations with West African Sequences, in *The West African Orogens and Circum-Atlantic Correlatives*, edited by R. D. Dallmeyer and J. P. Lécorché, pp. 267-293, Springer Berlin Heidelberg.

Ribeiro, A., et al. (2007), Geodynamic evolution of the SW Europe Variscides, *Tectonics*, 26, TC6009.

Ries, A. C. (1979), Variscan metamorphism and K-Ar dates in the Variscan fold belt of S Brittany and NW Spain, *Journal of the Geological Society*, 136(1), 89-103.

Rodríguez-Alonso, M. D., M. Peinado, M. Lopez-Plaza, P. Franco, A. Carnicero, and J. C. Gonzalo (2004), Neoproterozoic-Cambrian synsedimentary magmatism in the Central Iberian Zone (Spain): geology, petrology and geodynamic significance, *International Journal of Earth Sciences*, 93, 897-920.

Romeo, I., R. Lunar, R. Capote, C. Quesada, R. Piña, G. R. Dunning, and L. Ortega (2006), U-Pb age constraints on Variscan magmatism and Ni-Cu-PGE metallogeny in the Ossa-Morena zone (SW Iberia), *Journal of the Geological Society*, 163, 837-846.

Rubio-Ordóñez, A., P. Valverde Vaquero, L. G. Corretge, A. Cuesta-Fernández, G. Gallastegui, M. Fernández-González, and A. Gerdes (2012), An Early Ordovician tonalitic–granodioritic belt along the Schistose-Greywacke Domain of the Central Iberian Zone (Iberian Massif, Variscan Belt), *Geological Magazine*, 149, 927-939.

Rubio-Ordóñez, A., G. Gutiérrez-Alonso, P. Valverde-Vaquero, A. Cuesta, G. Gallastegui, A. Gerdes, and V. Cárdenes (2015), Arc-related Ediacaran magmatism along the northern margin of Gondwana: Geochronology and isotopic geochemistry from northern Iberia, *Gondwana Research*, 27, 216-227.

Sánchez-Carretero, R., M. Carracedo, L. Eguiluz, A. Garrote, and O. Apalategui (1989), El magmatismo calcoalcalino del Precámbrico terminal en la Zona de Ossa–Morena (Macizo Ibérico), *Revista de la Sociedad Geológica de España*, 2(1-2), 7-21.

Sánchez-García, T., F. Bellido, and C. Quesada (2003), Geodynamic setting and geochemical signatures of Cambrian–Ordovician rift-related igneous rocks (Ossa-Morena Zone, SW Iberia), *Tectonophysics*, 365, 233-255.

Sánchez-García, T., C. Quesada, F. Bellido, G. R. Dunning, and J. González del Tánago (2008), Two-step magma flooding of the upper crust during rifting: The Early Paleozoic of the Ossa Morena Zone (SW Iberia), *Tectonophysics*, 461, 72-90.

Sánchez-García, T., F. Bellido, M. F. Pereira, M. Chichorro, C. Quesada, C. Pin, and J. B. Silva (2010), Rift-related volcanism predating the birth of the Rheic Ocean (Ossa-Morena zone, SW Iberia), *Gondwana Research*, *17*, 392-407.

Sánchez-García, T., C. Quesada, F. Bellido, G. R. Dunning, C. Pin, E. Moreno-Eiris, and A. Perejón (2016), Age and characteristics of the Loma del Aire unit (SW Iberia): Implications for the regional correlation of the Ossa-Morena Zone, *Tectonophysics*, *681*, 58-72.

Sánchez-García, T., M. F. Pereira, F. Bellido, M. Chichorro, J. B. Silva, P. Valverde-Vaquero, C. Pin, and A. R. Solá (2014), Early Cambrian granitoids of North Gondwana margin in the transition from a convergent setting to intra-continental rifting (Ossa-Morena Zone, SW Iberia), *International Journal of Earth Sciences*, *103*, 1203-1218.

Sánchez-Lorda, M. E., B. Ábalos, S. García de Madinabeitia, L. Eguíluz, J. I. Gil Ibarra, and J. L. Paquette (2016), Radiometric discrimination of pre-Variscan amphibolites in the Ediacaran Serie Negra (Ossa-Morena Zone, SW Iberia), *Tectonophysics*, *681*, 31-45.

Sánchez Lorda, M. E., F. Sarrionandia, B. Ábalos, M. Carracedo, L. Eguíluz, and J. I. Gil Ibarra (2014), Geochemistry and paleotectonic setting of Ediacaran metabasites from the Ossa-Morena Zone (SW Iberia), *International Journal of Earth Sciences*, *103*(5), 1263-1286.

Schäfer, H.-J., D. Gebauer, T. F. Nägler, and L. Eguíluz (1993), Conventional and ion-microprobe U-Pb dating of detrital zircons of the Tentudía Group (Serie Negra, SW Spain): implications for zircon systematics, stratigraphy, tectonics and the Precambrian/Cambrian boundary, *Contributions to Mineralogy and Petrology*, *113*, 289-299.

Schäfer, H. J. (1990), Geochronological investigations in the Ossa-Morena Zone, SW Spain, PhD. thesis, 153 pp, ETH, Zurich.

Shelley, D., and G. Bossière (2000), A new model for the Hercynian Orogen of Gondwanan France and Iberia, *Journal of Structural Geology*, 22, 757-776.

Silva, J. B., and M. F. Pereira (2004), Transcurrent continental tectonics model for the Ossa-Morena Zone Neoproterozoic-Paleozoic evolution, SW Iberian Massif, Portugal, *International Journal of Earth Sciences*, 93, 886-896.

Simancas, F., I. Expósito, A. Azor, D. Martínez Poyatos, and F. González Lodeiro (2004), From the Cadomian orogenesis to the Early Palaeozoic Variscan rifting in Southwest Iberia, *Journal of Iberian Geology*, 30, 53-71.

Simancas, J. F., A. Azor, D. Martínez-Poyatos, A. Tahiri, H. El Hadi, F. González-Lodeiro, A. Pérez-Estaún, and R. Carbonell (2009), Tectonic relationships of Southwest Iberia with the allochthons of Northwest Iberia and the Moroccan Variscides, *Comptes Rendus Geoscience*, 341, 103-113.

Simancas, J. F., et al. (2003), Crustal structure of the transpressional Variscan orogen of SW Iberia: SW Iberia deep seismic reflection profile (IBERSEIS), *Tectonics*, 22, 1062.

Stampfli, G. M., C. Hochard, C. Vérard, C. Wilhem, and J. vonRaumer (2013), The formation of Pangea, *Tectonophysics*, 593, 1-19.

Stern, R. J. (2002), Subduction zones, *Reviews of Geophysics*, 40(4), 3-1-3-38.

Stern, R. J., and S. H. Bloomer (1992), Subduction zone infancy: Examples from the Eocene Izu-Bonin-Mariana and Jurassic California arcs, *Geological Society of America Bulletin*, 104(12), 1621-1636.

Strachan, R. A., and G. K. Taylor (1990), *Avalonian and Cadomian Geology of the North Atlantic*, London.

Taira, A. (2001), Tectonic Evolution of the Japanese Island Arc System, *Annual Review of Earth and Planetary Sciences*, 29(1), 109-134.

Talavera, C., D. Martínez Poyatos, and F. González Lodeiro (2015), SHRIMP U–Pb geochronological constraints on the timing of the intra-Alcudian (Cadomian) angular unconformity in the Central Iberian Zone (Iberian Massif, Spain), *International Journal of Earth Sciences*, 104(7), 1739-1757.

Taylor, B., and G. D. Karner (1983), On the evolution of marginal basins, *Reviews of Geophysics*, 21(8), 1727-1741.

Uyeda, S., and H. Kanamori (1979), Back-arc opening and the mode of subduction, *Journal of Geophysical Research: Solid Earth*, 84(B3), 1049-1061.

Valle Aguado, B., M. R. Azevedo, U. Schaltegger, J. R. Martínez Catalán, and J. Nolan (2005), U–Pb zircon and monazite geochronology of Variscan magmatism related to syn-convergence extension in Central Northern Portugal, *Lithos*, 82, 169-184.

Villaseca, C., E. Merino, R. Oyarzun, D. Orejana, C. Pérez-Soba, and E. Chicharro (2014), Contrasting chemical and isotopic signatures from Neoproterozoic metasedimentary rocks in the Central Iberian Zone (Spain) of pre-Variscan Europe: Implications for terrane analysis and Early Ordovician magmatic belts, *Precambrian Research*, 245, 131-145.

Wakabayashi, J., and Y. Dilek (2003), What constitutes ‘emplacement’ of an ophiolite?: Mechanisms and relationship to subduction initiation and formation of metamorphic soles, *Geological Society, London, Special Publications*, 218(1), 427-447.

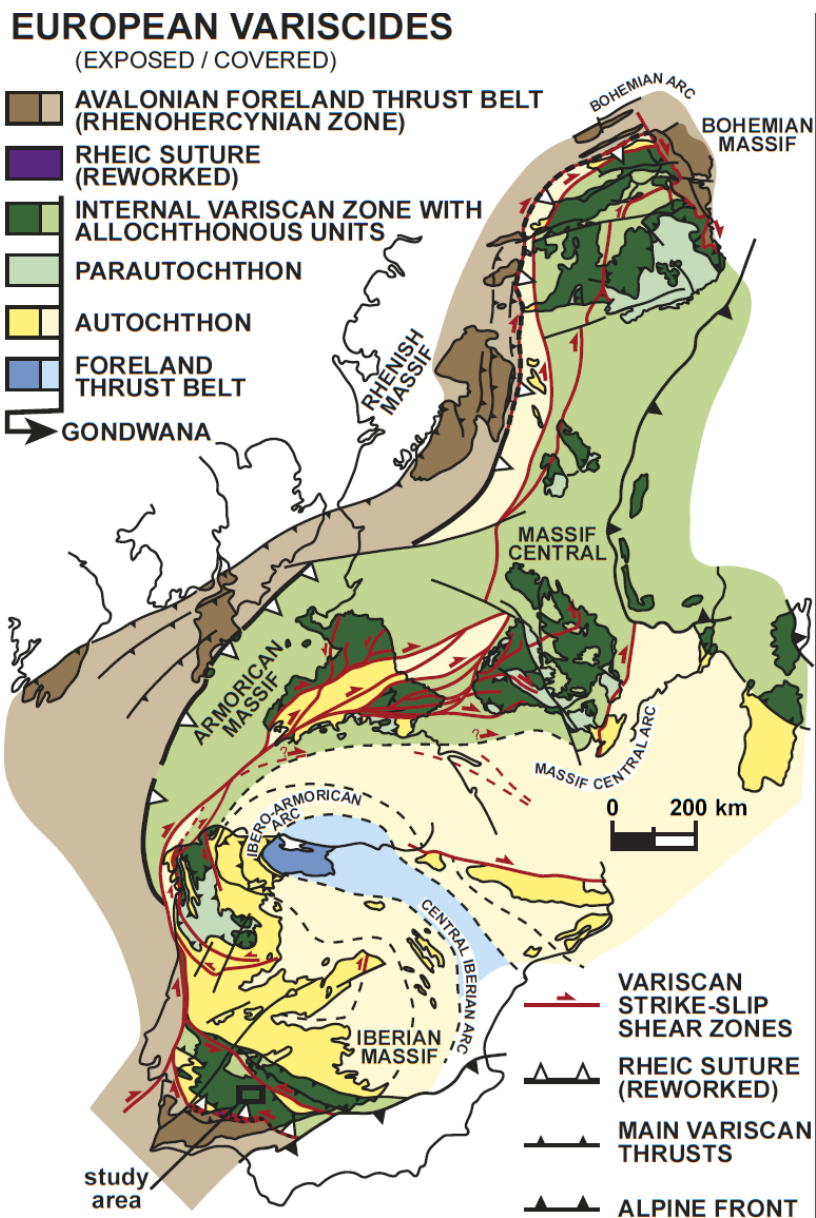


**Figure 1.** Location of the study area shown in a paleogeographic reconstruction of the Variscan orogen [Díez Fernández and Arenas, 2015]. Present European coastlines are included for georeference.

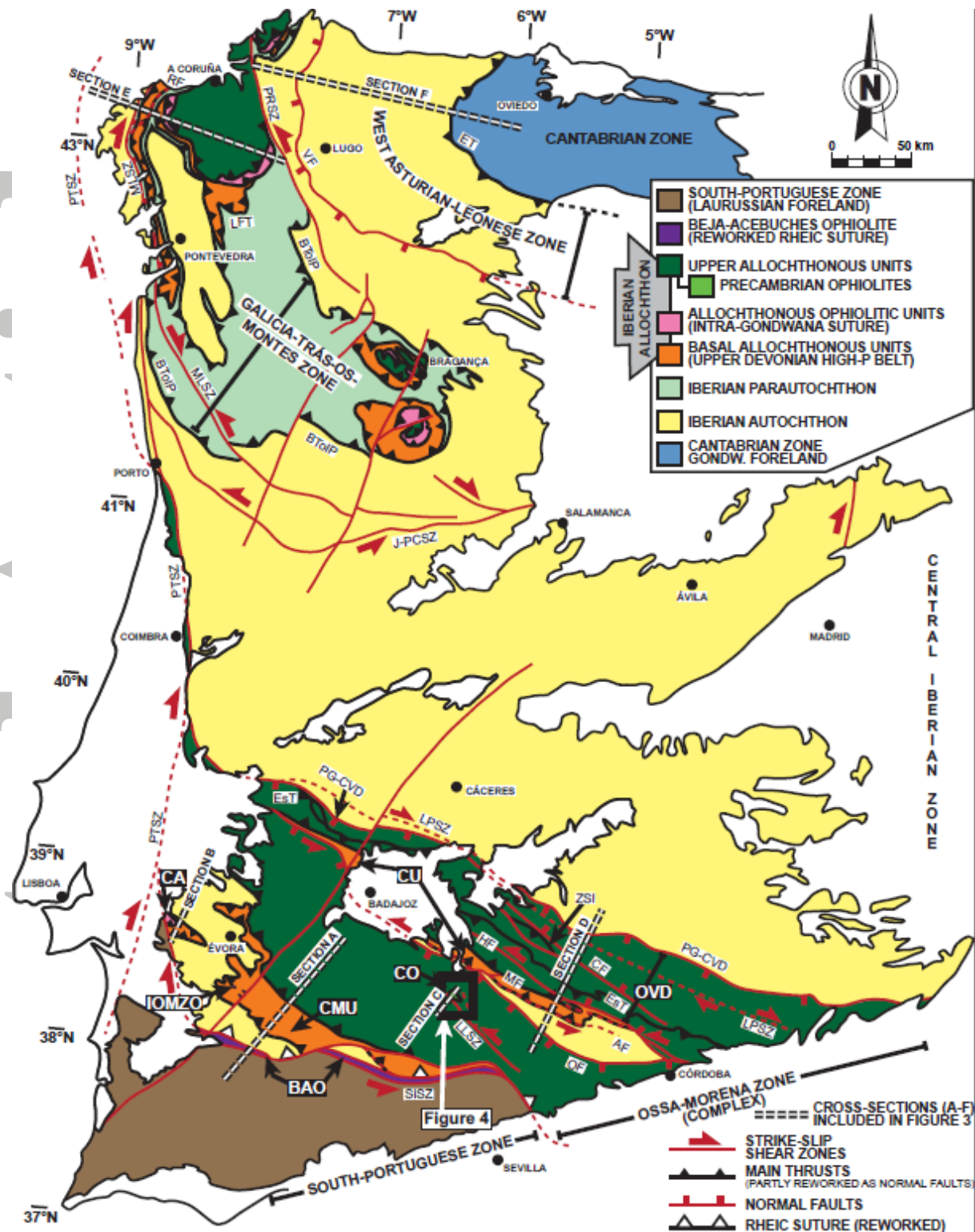


**Figure 2.** Geological map of the Iberian Massif [Díez Fernández and Arenas, 2015] indicating the location of the study area. Abbreviations: AF — Azuaga Fault; BT oIP — Basal

Thrust of the Iberian Parautochthon; BAO — Beja–Acebuches Ophiolite; CA — Carvalho Amphibolites; CF — Canaleja Fault; CMU — Cubito–Moura Unit; CO — Calzadilla Ophiolite; CU — Central Unit; EsT — Espiel Thrust; ET—Espina Thrust; HF— Hornachos Fault; IOMZO — Internal Ossa-Morena Zone Ophiolites; J-PCSZ — Juzbado-Penalva do Castelo Shear Zone; LFT — Lalín-Forcarei Thrust; LPSZ — Los Pedroches Shear Zone; LLSZ — Llanos Shear Zone; MLSZ — Malpica–Lamego Shear Zone; MF — Matachel Fault; OF— Onza Fault; OVD — Obejo–Valsequillo Domain; PG–CVD — Puente Génave–Castelo de Vide Detachment; PRSZ— Palas de Rei Shear Zone; PTSZ — Porto–Tomar Shear Zone; RF — Riás Fault; SISZ — South Iberian Shear Zone; VF — Viveiro Fault; ZSI — Zalamea de la Serena Imbricates.

Accepted Article

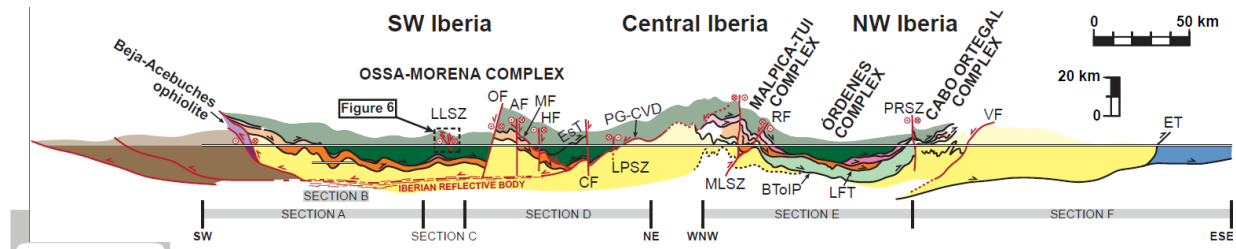


**Figure 3.** Composite cross-section of major tectonic elements of the Iberian Massif [after Díez Fernández and Arenas, 2015]. Abbreviations follow Figure 2.

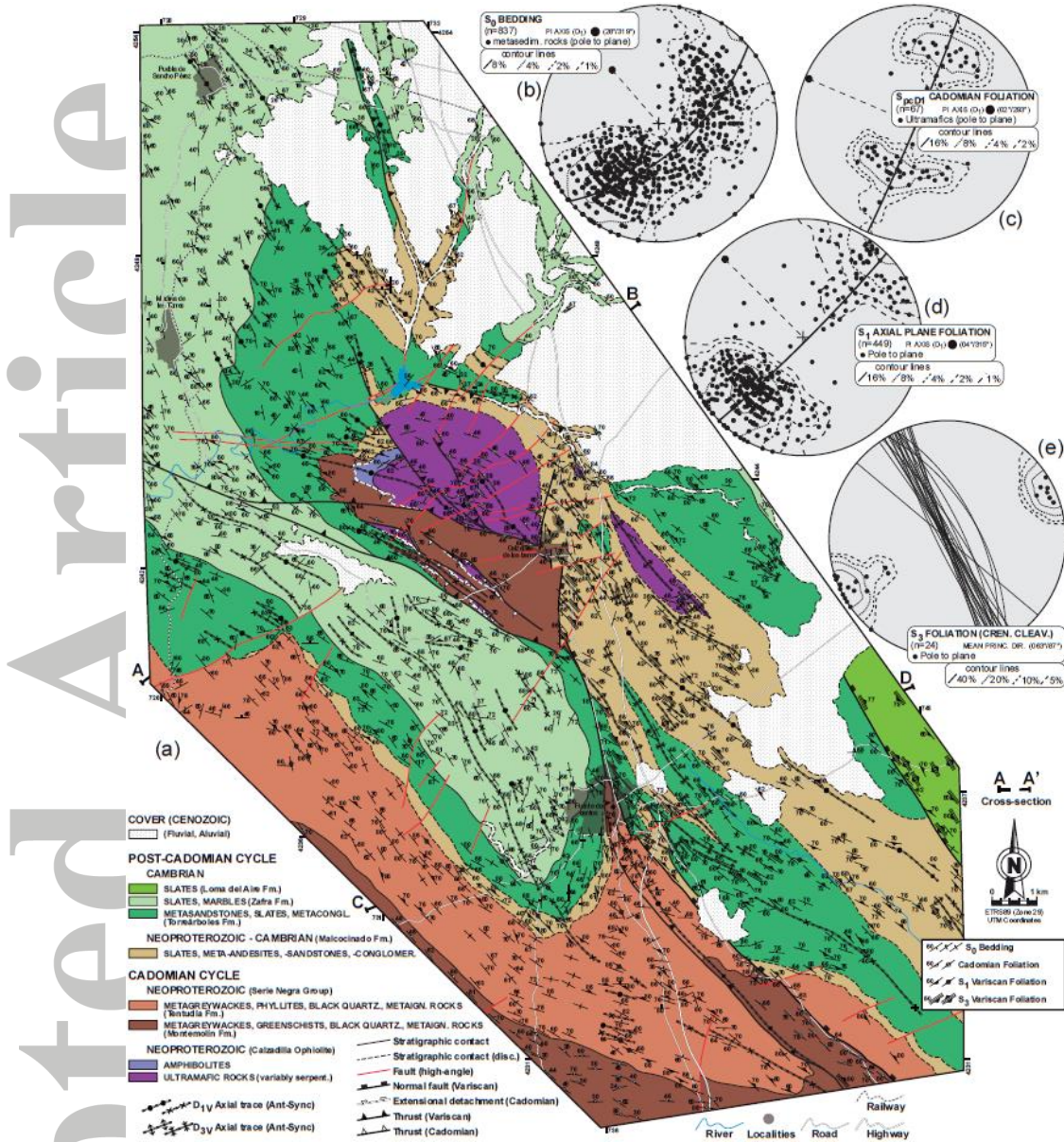


**Figure 4.** (a) Geological map of the study area with planar structural data. Bedding measurements ( $S_0$ ) in the Serie Negra Group are parallel to  $S_{pcD1}$ . Location of cross sections in Figure 6 is indicated. (b)  $\pi$ -diagram to calculate  $D_1$  axis orientation using bedding. (c)  $\pi$ -diagram to calculate  $D_1$  axis orientation using  $S_{pcD1}$  from metaultramafic rocks NW of Calzadilla de los Barros village. (d)  $\pi$ -diagram to calculate  $D_1$  axis orientation using axial planar  $S_1$ . (e) Stereoplot of  $S_3$ . Stereoplots are equal angle, lower hemisphere.

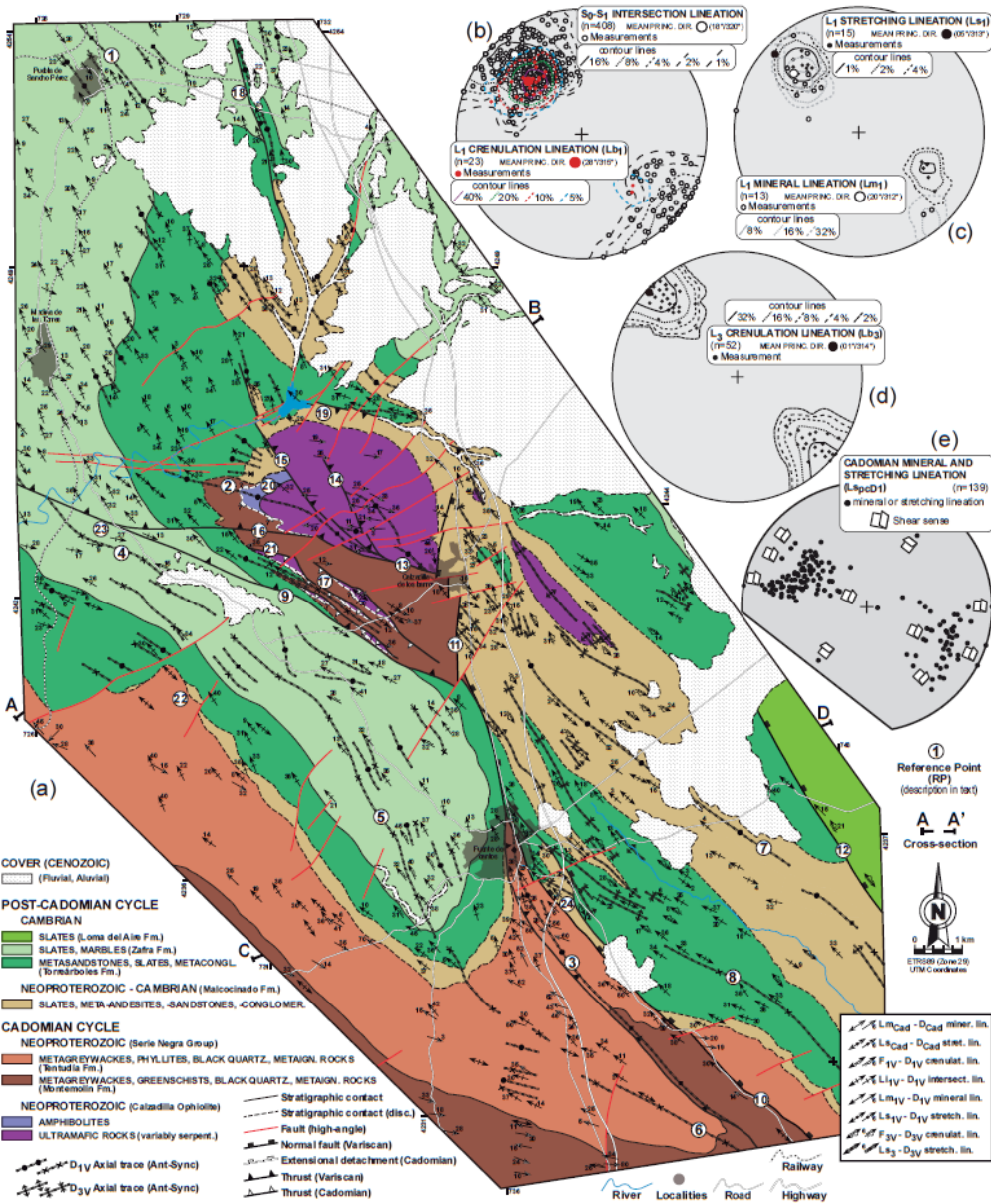


**Figure 5.** (a) Geological map of the study area with linear structural data. Circled numbers refer to key sites for understanding the regional structure (see text for explanation). Names of the main structures are provided. (b) Stereoplot including  $S_0$ - $S_1$  intersection lineation and crenulation lineation (observed in  $S_{pcD1}$ ). (c) Stereoplot of  $D_1$  stretching ( $L_{s1}$ ) and mineral lineations ( $L_{m1}$ ). (d) Stereoplot showing  $D_3$  crenulation lineation ( $L_{b3}$ ). (e) Stereoplot with Cadomian mineral and stretching lineation ( $L_{pcD1}$ ), and shear sense criteria. Plots are equal angle, lower hemisphere.

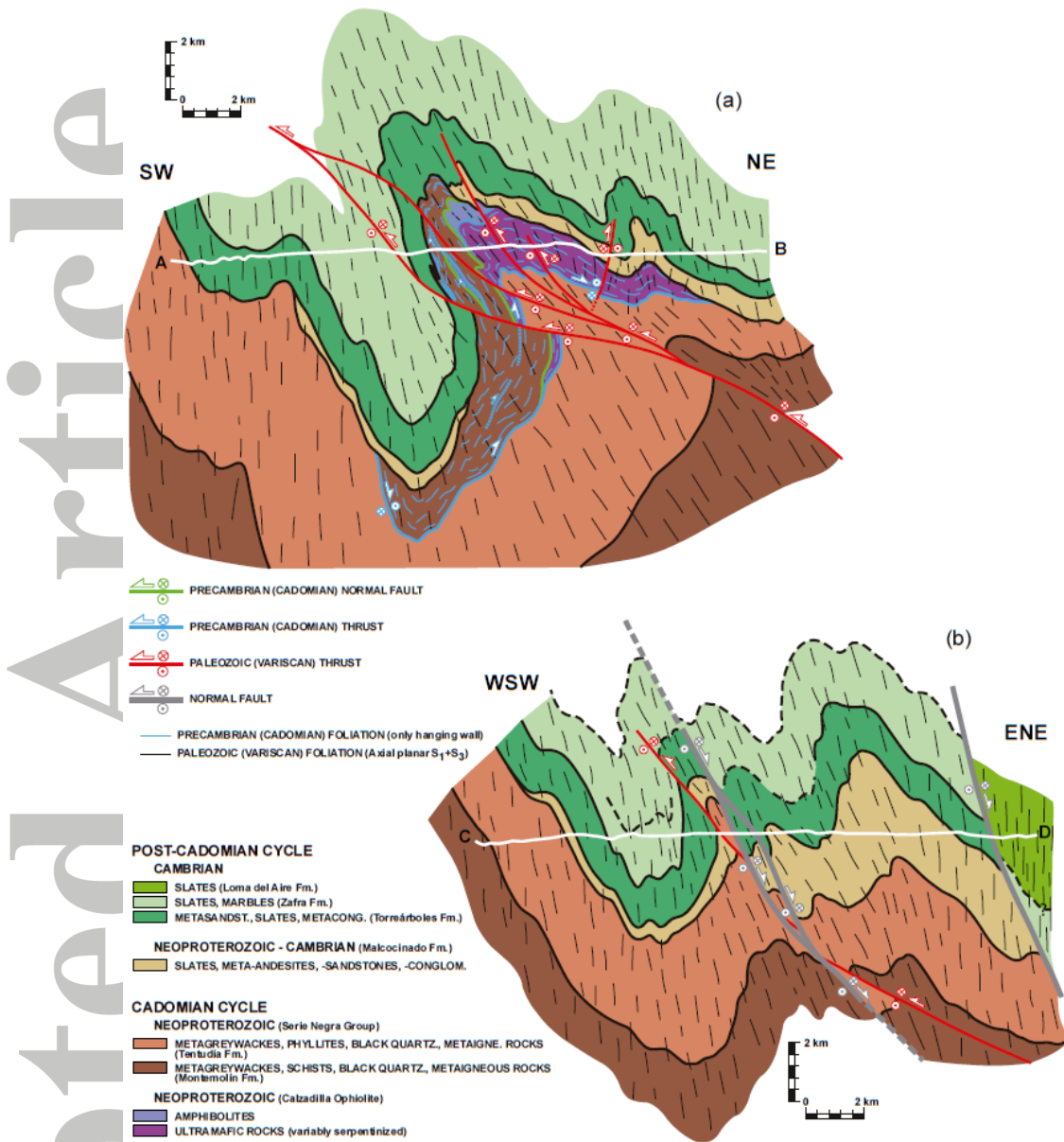


**Figure 6.** Representative cross-sections across the study area. Location of the section in the northern part (a) and in the southern part (b) are indicated in Figure 4.

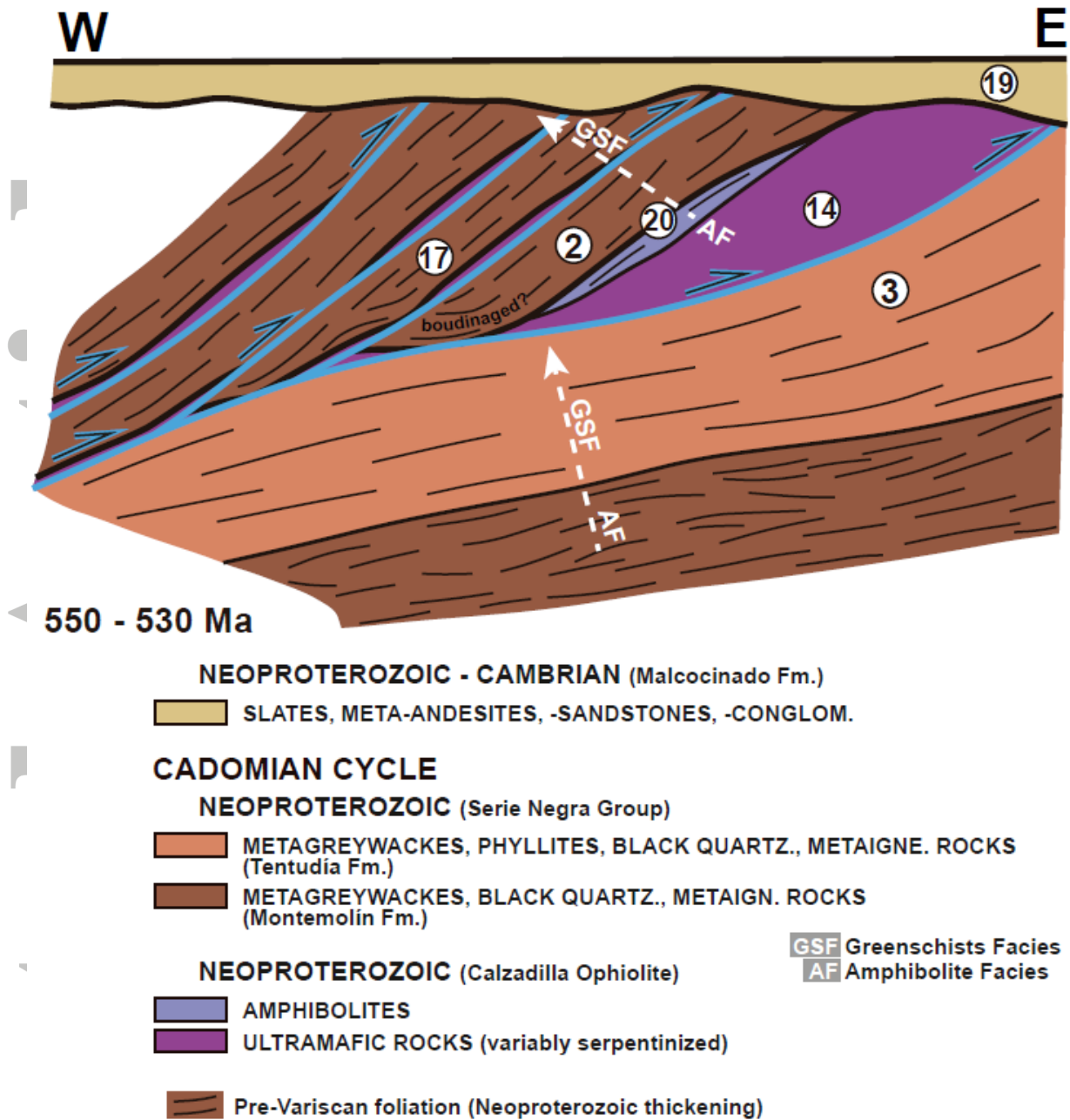


**Figure 7.** Simplified reconstruction of the Ediacaran structure (not-to-scale). Circled numbers refer to reference points (RP) indicated in Figure 5a. Cadomian metamorphic gradients are indicated with dashed, white arrows. Geographical coordinates correspond to present-day.

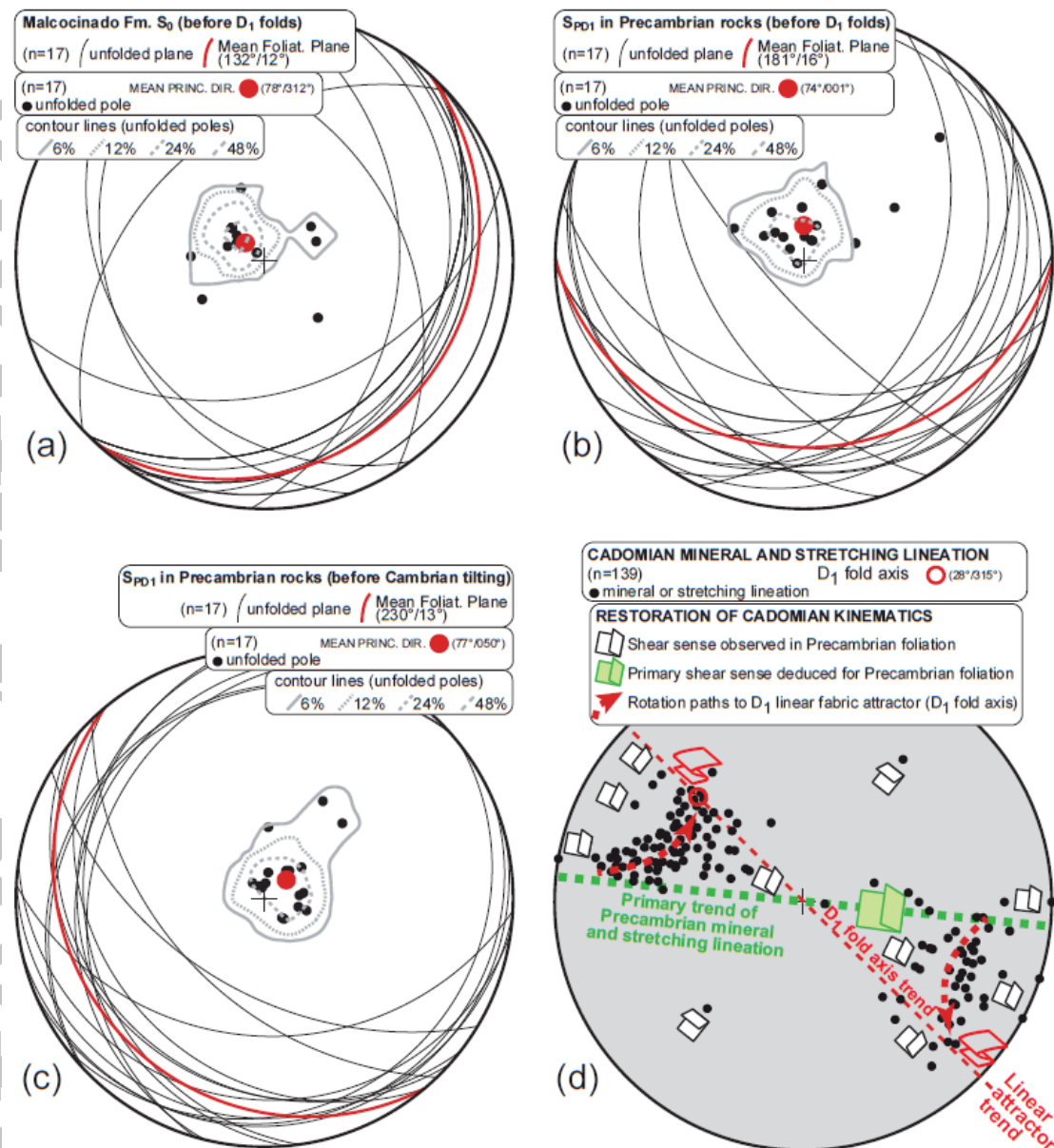


**Figure 8.** (a) Stereoplot showing the orientation of  $S_0$  in the Malcocinado Formation after unstraining Variscan folding. (b) Similar stereoplot for Cadomian foliation ( $S_{pcD1}$ ) in the Serie Negra Group. (c) Stereoplot showing the primary orientation of  $S_{pcD1}$  in the Serie Negra Group after unstraining Cambrian tilting. (d) Stereoplot of Cadomian mineral and stretching lineations ( $L_{S_{pcD1}}$ ) alongside the orientation and trend of regional  $D_1$  fold axis (calculated in Fig. 5b). Green dashed line indicates the primary trend of Cadomian lineations as deduced from their reorientation path towards  $D_1$  fold axis (linear fabric attractor). Plots are equal angle, lower hemisphere.

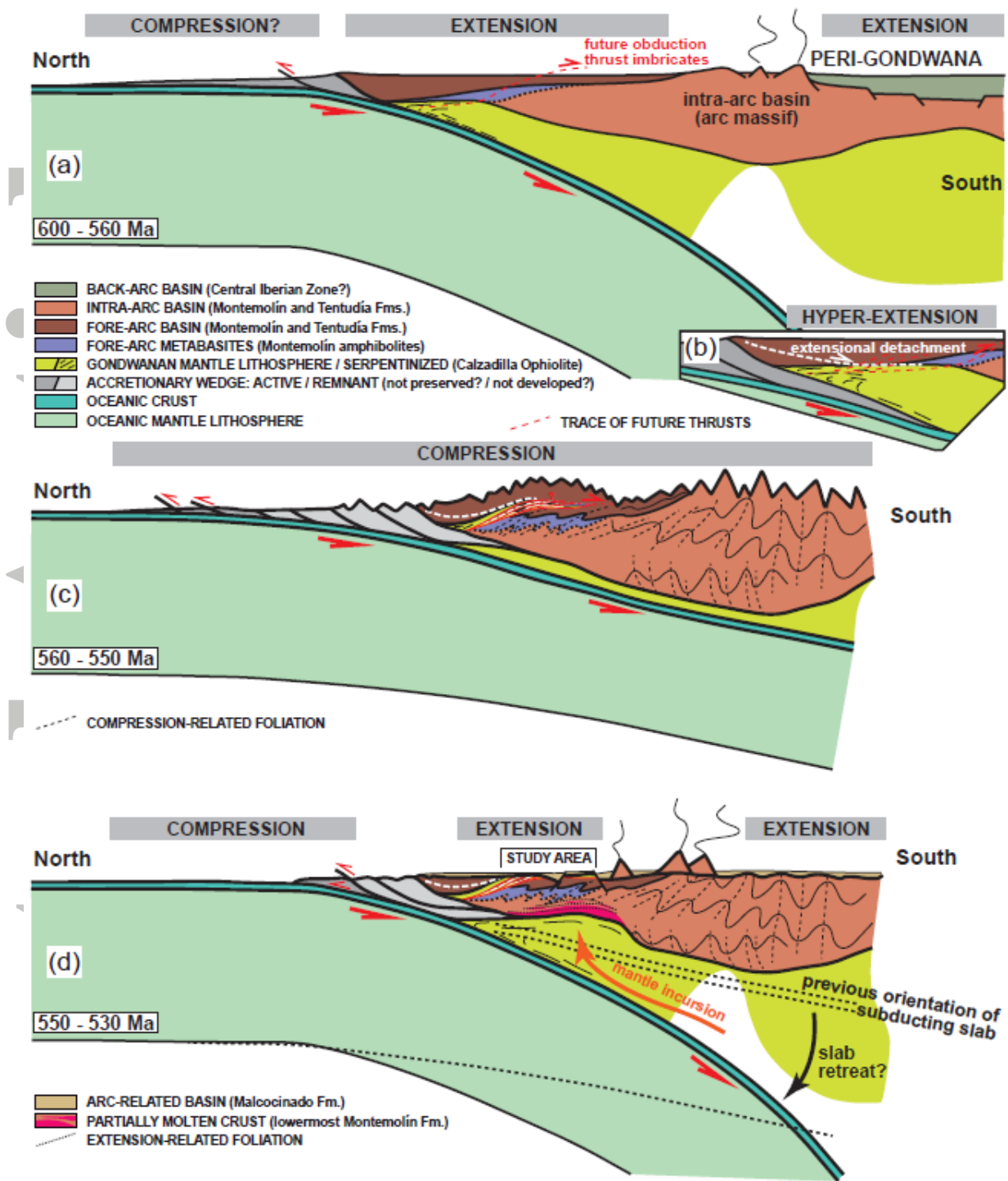


**Figure 9.** Tectonic model for the Ediacaran and Cambrian evolution of the northern margin of Gondwana as inferred from this study (see discussion and explanation in main text). Paleogeographic coordinates.